



Master Thesis
MAS500

MR Damper hysteresis characterization for the semi-active
suspension system

Dariush Ghorbany

Supervisors

Hamid Reza Karimi

Yousef Iskandarani

University of Agder, 2011

Faculty of Engineering and Science

Department of Engineering

Abstract

This thesis presents the nonlinear MR brake to a semi active suspension system (e.g. of a vehicle suspension). Semi-active control has recently received considerable attention in some years, because its strong potential to control devices without imposing heavy power demands.

The dynamic response characteristics of the damper are captured in data collection, random input signals were used for angular velocity and current input.

The relationship between the current and damping force in magneto-rheological brake is nonlinear but in the reality it is possible to control the current of MR brake to reduce the vibration of the system as much as possible, because the nonlinearity of the model depends on the current and angular velocity.

The first part of this project describes the vibration suppression in passive, active and semi active suspension. Subsequently several mathematical models are used to simulate and analyze hysteresis behavior of magneto-rheological brake. The second part of this work is devoted to derivation of the dynamic model equation of the experimental setup. The last part presents the evaluation of the dynamic simulation modeling results with the full-scale experimental data. In particular, special attention is paid to comparison with the Bouc-Wen model analysis.

Acknowledgements

I would like to express my gratitude to my supervisor, Professor Hamid Reza Karimi for his valuable support through my Master's studies. I believe his guidance will be influential throughout the rest of my career.

I would also like to thank the assistant supervisor, Yousef Iskandarani who helped me during realization of the experimental part of this project.

Contents

Abstract	2
Acknowledgements	3
Contents	4
List of figures	6
List of tables	7
Nomenclature.....	8
1. Introduction.....	9
1.1 Objective.....	10
1.2 Organization	10
2 Vibration suppression.....	11
2.1 Passive suspension	12
2.2 Active suspension	14
2.3 Semi active suspension system	15
3 Physical study	18
3.1 Magneto-rheological braking	18
3.2 MR brake magnetic model	19
3.3 MR fluid	21
4 SAS system.....	23
4.1 Introduction.....	23
4.1.1 Purpose.....	23
4.1.2 System description	23
4.2 Components	24
4.2.1 Encoder.....	24
4.2.2 Body.....	26
4.2.3 Body calculation geometry.....	27
4.2.4 Spring calculation	27
4.2.5 Tire elasticity	30
4.2.6 Linear movement calculation	31
4.3 Geometry Torque Representation	33
4.3.1 Upper beam Analysis.....	33
4.3.2 Lower beam Analysis	35
4.4 Real experimental data	38
4.4.1 Experimental Damping	40

- 5 Identification 42
 - 5.1 Parameters Estimation 42
 - Bouc-Wen model..... 45
 - 5.1.1.1 Parameters Analysis 46
 - Parameters Identification..... 47
 - 5.1.2 Dahl model 49
 - 5.1.2.1 Parameters Analysis 50
 - 5.1.2.2 Parametrs Identification..... 51
 - 5.1.3 Bingham model..... 52
 - 5.1.3.1 Parameters Analysis 53
 - 5.1.3.2 Parameters Identification..... 54
- 6 Electronic setup 55
 - 6.1 Signals in/out..... 55
 - 6.1.1 Motors 56
 - 6.1.2 Cam follower system (Eccentric) 56
 - 6.1.3 Wheel 58
 - 6.1.4 Mass and unsprung mass 58
 - 6.1.5 Brake..... 58
 - 6.2 Connection diagram 59
- 7 Software setup 60
 - 7.1 Design of semi active controller..... 60
 - 7.2 RT (SAS)..... 61
 - 7.3 Modules..... 62
- 8. Project conclusion 64
 - 8.1 Future work 64

List of figures

Figure 2.1	Overview of vibration suppression	11
Figure 2.1 1	Passive system in structure building	12
Figure 2.1. 2	Passive suspension	13
Figure 0.2	Active mass damper (AMD system)	14
Figure 1.3. 1	Tuned mass damper (TMD)	15
Figure 2.3. 2	Tuned liquid damper(TLD)	15
Figure 2.3. 3	Semi Active Suspension system	16
Figure 2.3. 4	Simulation results in passive and semi-active	17
Figure 3.1	MR Rotary brake	18
Figure 3.2	Linear MR damper	18
Figure 3.2. 1	MR brake structure with the form of rotary disks	19
Figure 3.2. 2	MR Brake Disassembled and Assembled	19
Figure 3.2. 3	Block diagram for nonlinear model of the MR brake	20
Figure 3.2. 4	Structure of MR Rotary damper	20
Figure 3.3. 1	Magnetorheological fluid	20
Figure 3.3. 2	MR fluid in valve mode	22
Figure 3.3. 3	MR fluid in Direct-shear Mode	22
Figure 3.3. 4	MR fluid in Squeeze Mode	22
Figure 4.2. 1	Encoder of the experimental setup behind of MR brake	24
Figure 4.2. 2	Simulink block diagram of encoder in experimental setup	25
Figure 4.2. 3	Encoders Simulink result	25
Figure 4.2. 4	Geometrical diagram of semi active system	26
Figure 4.2. 5	Body Geometry	27
Figure 4.2. 6	Spring Geometry	27
Figure 4.2. 7	Pythagorean calculation of spring due to the body	28
Figure 4.2. 8	Pythagorean calculation of spring due to the unsprung mass	28
Figure 4.2. 9	Linear movement calculation	31
Figure 4.3. 1	Upper beam Analysis	33
Figure 4.3. 2	Gravitational moment of lowerbeam	35
Figure 4.4.1	Simulation result of real experimental data	39
Figure 4.4.2	Excitation input	39
Figure 4.4.3	Damping coefficient of MR brake	40
Figure 4.4.4	Damping simulation of MR brake	41
Figure 5.1. 1	Estimation method	41
Figure 5.1. 2	Simulink dynamic model	43
Figure 5.1.3	Bouc-Wen model approximation	43
Figure 5.1.4	Bingham model approximation	44
Figure 5.1.5	Dahl model approximation	44
Figure 5.1.6	Bouc-Wen Model of the MR Damper	45
Figure 5.1. 7	Dynamic characteristic Torque-Angular velocity	46
Figure 5.1. 8	Dynamic characteristics Torque-Displacement	46
Figure 5.1. 9	Simulink block diagram of Bouc-Wen model	47
Figure 5.1. 10	Identification Torque-Angular velocity and Torque-Angle	47
Figure 5.1. 12	Torque-Time	48
Figure 5.2. 2	Simulink diagram of function of torque due to the MR brake	49
Figure 5.2. 3	Torque – Angular velocity (deg/sec)	50
Figure 5.2. 4	Torque – Angle(deg)	50
Figure 5.2. 5	Simulation result parameters of Dahl model	51
Figure 5.3. 1	Bingham Model of a Controllable Fluid	52
Figure 5.3.2	Simulink diagram of Bingham	52

Figure 5.3. 3	Torque – Angle (Deg)	53
Figure 5.3. 4	Torque – Angular velocity (Deg/sec)	53
Figure 5.3. 5	Simulation results of Bingham	54
Figure 6. 1	Electronic setup of semi active	56
Figure 6. 2	Cam Design	57
Figur 6. 3	Quarter of car design	58
Figure 6. 4	Picture of MR brake	59
Figure 6.2.1	Prototype of the semi-active friction device	60
Figur 6.2. 2	MR Damper Feedback Control	60
Figure 7.2. 1	Real time of SAS	62
Figure 7.3.1	Control window of SAS	63
Figure 7.3. 2	Real-time Device Driver	63
Figure 7.3. 4	Simulation model of the SAS	64
Figure 7.3. 5	ABS device Driver	65

List of tables

Table 1	Bouc-Wen model parameters	47
Table 2	Dahl model parameters	50

Nomenclature

Parameters	Description	Unit
C	Rotary damper	
k_g	Linear stiffness	$[Nm^{-1}]$
k_s	Elasticity coefficient	$\left[\frac{N}{m}\right]$
f_g	Absorption coefficient	$\left[\frac{Ns}{m}\right]$
I	Current	$[A]$
T_{MR}	Torque MR damper	$[Nm]$
G	Gravitation	$\left[\frac{m}{s^2}\right]$
α_1, α_2	Angle	$[Deg]$
m_s, m_u	Mass / unsprung mass	$[kg]$
r_1, r_2	Distance	$[m]$
l_{0s}	length of the no load spring	$[m]$
G_2	Gravitaional forces of body	$[N]$
\dot{x}	Derivation displacement of tire elasicity	$\left[\frac{m}{s}\right]$
$\dot{\theta}$	Angular velocity	$\left[\frac{Deg}{sec}\right]$
θ	Angle	$[Deg]$
f_c	Friction force	$[N]$
c_0	Damping coefficient	$\left[\frac{Ns}{m}\right]$

Description

SAS	Semi Active Suspension
$k_{w_a}, k_{w_b}, k_{x_a}, k_{x_{wb}}$	Dahl model parameters
$C_0, C_1, \alpha_0, \alpha_1$	Bouc-Wen model parameters
I/O	Input/Output

Symbols

$\alpha, \beta, \gamma, n, \delta$	Non dimensional parameters of Bouc-Wen model
ρ	Non dimensional parameters of Dahl model
f_0	Non zero

1. Introduction

The purpose of this project is to provide the reader with information regarding different vibration suppression strategies, particularly SAS mechanical system's description and modeling. There are three main types of vehicle suspensions that have been proposed, that is, passive, semi-active and active suspensions, which depend on the operation mode to improve vehicle ride comfort, vehicle safety, road damage minimization and the overall vehicle performance. Study of vehicle vibration reduction in this project was made by simulating the dynamics of a semi active suspension system.

There are various mechanical systems in the world which provide isolation of a structure from the effect of disturbances (e.g. vibrations). One example of such a device is a rotational magneto-rheological brake (MR brake) which creates braking torque by changing the viscosity of the MR fluid inside the brake. The magneto-rheological brakes are used in many applications including prosthetics, automotive, vibration stabilization. In this project, there is presented examination of the mechanical system equipped with MR brake. The main aim of this thesis is to obtain the hysteresis plot by finding the torque in MR brake dependent on different input current. A passive suspension has the ability to store energy via a spring and to dissipate it via a damper. In the passive suspension system, the sprung mass, spring and damper parameters are generally fixed, and they already have been chosen in terms of the design requirements of this part of experimental setup. All the physical and geometrical constants characterizing the real experimental setup which is examined here were included and given in the SAS manufacturer's documentation.

1.1 Objective

This project provided with an introduction of semi active suspension by a mechanical system or experimental setup to test the hysteresis behavior with real data. And tries to evaluate the following main areas:

1. Study about vibration suppression. Such as passive, active and semi active.
2. Study the mechanical system of experimental setup, and write the dynamic equation of the SAS system.
3. Study about the torque in the MR brake.
4. Parameters estimation of the different mathematical model. Such as Bouc- Wen, Dahl and Bingham models.
5. Identification of the parameters.
6. To get the hysteresis of the experimental setup with real parameters, and compare with the others model.

1.2 Organization

This project presents some introduction of the vibration suppression system in three different strategy in chapter 2. Then the physical study of the Magnetor-rheological brake is explained in the chapter 3. Chapter 4 describe the theory of SAS physical system in geometrical and dynamic equation. In the chapter 5 the estimation and identification parameters of experimental setup will be done. Chapter 6 explain the electronic setup of each part of mechanical system. Chapter 7 explain about software setup, to shows how different SAS (such as Real Experimental Data, RPM Stabilization, Real Time Data, SAS Simulation) system works.

2 Vibration suppression

The process of vibration suppression system is in different categories step by step shows in figure 2.1.

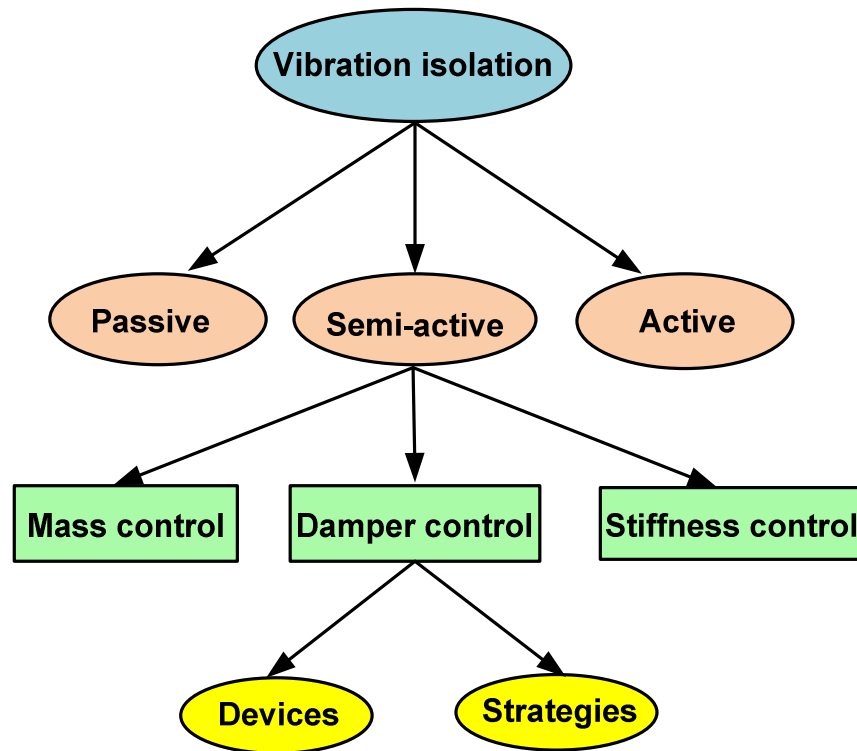


Figure 2-1 Overview of vibration suppression

The explanation of the figure 2.1 is that, there are three ways to prevent the vibration, as shown as above, and those are passive, active and semi active dampers.

Vibration suppression has recently received much attention due to many different engineering applications. Such as rotating turbine and helicopter blades, robot arms, vehicular propulsion system.

The experience has showed that, there were some problems with the passive and active dampers system under the work. And those systems could not the complete the engineering's structure. Later on the semi active control system has been founded in 1970. The semi-active control has a good acceptable performance.

It is by using spring damper(C), spring stiffness (K), and mass (m) to make a magic mathematic function to control the vibration, the only problem of the system is high nonlinearity.

This section provides an overview and to compare of the passive, active and semi active control and explain the system advantages and disadvantages.

2.1 Passive suspension

Passive damping was one of the first solutions proposed to reduce the vibration in civil structures.

In this case, the system shows the forces that are developed in response to the motion of structures.

Isolator method can be used in passive damper systems, and the disadvantage is that, the motion of the structure increase, and also the system is nonlinear dynamic. But the advantages in this system are that, there is no external power source in passive control system, and also no additional hardware needed. Tuned mass damper is one of the examples in passive control system, which there are some pictures below explain, what is going on in this part of system. [5]

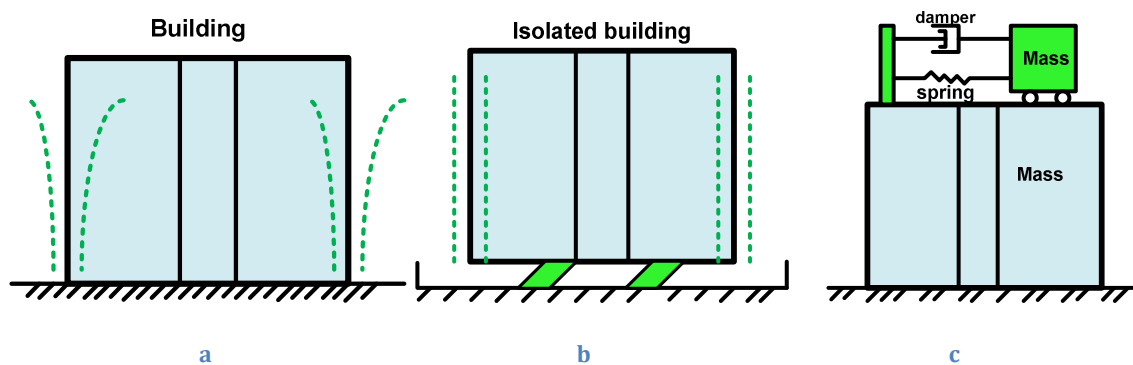


Figure 2.1. 1 Passive system in structure building

Where:

- a : Non isolate structure.
- b : The isolate structure.
- c : Is the tuned mass damper (TDM).

Here are some examples in buildings structures in passive suspension system, the buildings structure before and after isolating in passive suspension system.

In the figure (a) , building is ot isolated and it is on severe shaking, there is no control at all on this method.

The isolated buildings which shown as figure (b) is called seismic isolating, that is dependent on the ground.

The last one is called tuned mass damper, which is spring, damper and mass is installed on the top of structure, and it is in wind induced vibration control. [6]

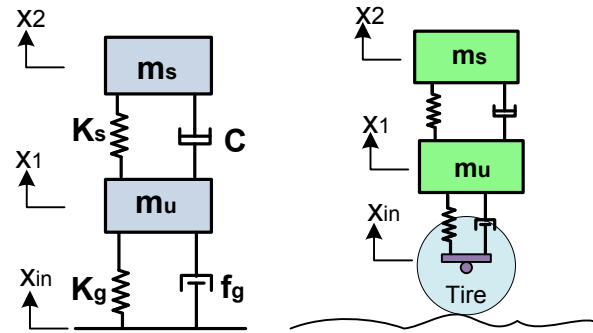


Figure 2.1.2 Passive suspension

- m_s : Sprung mass.
- m_u : Unsprung mass.
- k_s : Spring stiffness.
- k_g : Tire stiffness.
- f_g : Is the damping torque generated by the gum of tire.

A passive control system does not require an external power source.

A typical passive suspension can be modeled as shown in figure 2.1. 2 The input to this model is a displacement input which is representative of a typical road profile. The input x_{in} of system excites the first degree of freedom (the unsprung mass like a quarter of car, representing the wheel, tire, and some suspension components). The x_1 and x_2 is the displacement of the sprung mass and unsprung mass in vertical direction.

Passive systems include springs and passive dampers which reduce the vibration of the operator's bodies. But there is no control in the Magneto-rheological brake damping.

The passive suspension do not absorb forces applied to the system in the theoretical ways, but serve the purpose of dissipating energy from the vertical motion of the wheels and body.

$$T = C_{(i)}\dot{\theta} + \alpha_{(i)} z$$

$$C_{(i)} = C_0 + C_1 (i) \quad i = 0$$

$$\alpha_{(i)} = \alpha_0 + \alpha_1 (i) \quad i = 0$$

In passive suspension, there is no current (i) in the MR brake, it means that the parameters C_1 and α_1 are zero. In another case the mass/ body is in vibration when the wheel is running. Well in that case there is no control in the system, but still there is damping in the system even there is not current in the MR rotary brake, because of the parameters C_0 and α_0 . But the system is not controllable by current.

2.2 Active suspension

The response of structure in active control characterized by the following: first amount of external power or energy is required, and second a decision making process based on real time measured data is involved.

In an active control system, an external sources power control actuators that apply sources to structure.

Active vibration control of lightly damped and flexible structures such as high-rise buildings, to control buildings from earthquake has been widely researched.

In the other hands the active suspension is useful to support vehicle and isolates passengers from road disturbances for comfortable travel. Development of an active-suspension system should be accompanied by the methodologies to control it, but it is costly to consider a system active control.

The advantages in this system are that adaptable, and have better control performance, but the disadvantages are additional power needed, and external power required, and also the energy which can added, destabilize the system. [5]

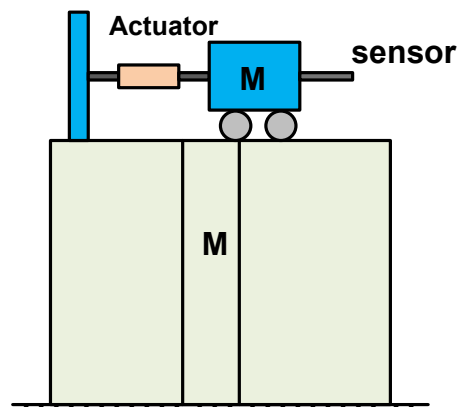


Figure 0.2 Active mass damper (AMD system)

In active mass damper (AMD), in this case, there is mass which is installed on the top of the structure, and it is connected to it by an actuator, and this mass is 1% less than total mass structure, and when the response of the whole structure is processed by the computer, then the computer can send the signals to the actuator to move the mass and to reduce the vibration. See figure 2.2.

2.3 Semi active suspension system

Semi-active control systems combine the best features of both approaches, offering the reliability of passive devices, and distinctly class of active control systems.

In this case, the external energy, are smaller than active control systems. The semi-active devices do not add the mechanical energy to the structural system, and are also viewed as controllable passive systems. Just to input the low power requirements, then there is a large controllable force capacity in the output. Therefore the semi-active strategies are a very good solution for civil engineering structures.

Semi-active systems can pass in three categories: and those are variable stiffness, variable damping and variable mass. As the mass cannot be changed in a short time, in most cases at the moment, only the first two are considered. In the first category, the systems stiffness is adjusted to establish a non-resonance condition. In the second category, semi-active devices are operated according to semi-active damping control strategies to generate a damping force passively. The MR damper is belongs to the two first categories, variable stiffness and variable damping. The objective of semi-active control is to reduce the vibrations.

Experience has shown that the semi-active damping systems perform better than passive and fully active systems and have the potential to achieve. In the other hands here there are some advantages and disadvantages of the semi active control:

The advantages are: comparable control performance to active control can adapt to varying loading conditions, do not needed to much power to operate, and the energy don't coming to the system to failure system.

The disadvantage is: it is only mathematically complex dynamic.

Some examples in semi-active devices include the controllable friction devices, controllable fluid dampers. [5]

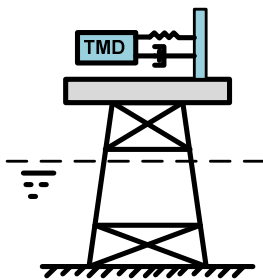


Figure 2.3. 1 Tuned mass damper (TMD)

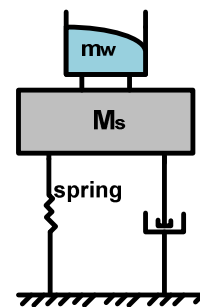


Figure 2.3. 2 Tuned liquid damper(TLD)

Tuned liquid dampers (TLD), which is the tuned liquid dampers, are economical and effective dynamic vibration absorbers. They have been increasingly used to control the dynamic response and protect structures from damage due to external excitations. The advantages of TLDs, is they can use for both small wind and large amplitude earthquake. They are easy to install, and the require is simple, and is not too expensive to require. TMD system is an acceptable strategy to control flexible structures, and particularly for tall buildings.

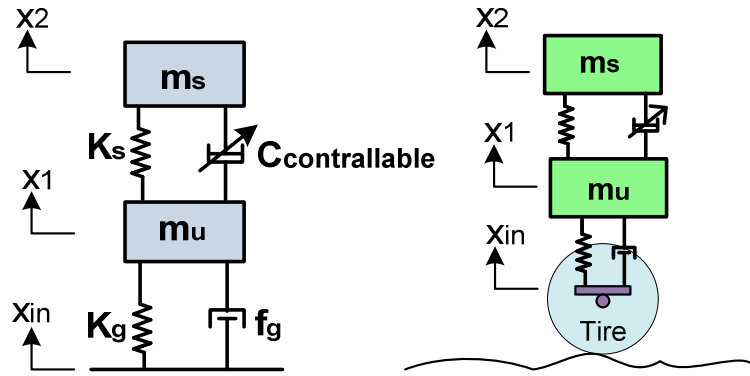


Figure 2.3. 3 Semi Active Suspension system

Semi-active damping control for vibration isolation is the subject of this thesis which is given better results damping vibrations. Typically, semi-active control devices do not add mechanical energy to the structural system.

The most common vibration place in to system is the absorption between the tire and the cam (Eccentric). The semi active suspension is called one degree of freedom (1DOF), since the rotation of MR brake.

The defining advantages of semi-active systems are that they can only dissipate energy and not create energy. Semi-active systems can use springs and active rotary brake which generally use magneto-rheological (MR) fluid to actively damping vibrations.

These suspension system works like the following way, a sensor detects the body's vibration, and a controller controls the flow and timing of fluid through the active MR brake to reduce the vibration of the body as much as possible.

These body suspension systems generally have springs and dampers, but their defining characteristic is that the active actuators can dissipate energy, as well as create energy. The ability to dissipate and create energy allows for greater vibration attenuation in the low-frequency rang.

The suspension system is represented by a linear spring of stiffness k_s and a rotational damper with a damping rate C . The tire is modeled by a linear spring of stiffness k_g and a linear damper with a damping rate f_g .

$$T = C_{(i)}\dot{\theta} + \alpha_{(i)} z$$

$$C_{(i)} = C_0 + C_1 (i) \quad i \neq 0$$

$$\alpha_{(i)} = \alpha_0 + \alpha_1 (i) \quad i \neq 0$$

In semi active suspension, the current (i) exists in the MR brake, it means that the parameters C and α are not zero. In this case the vibration of the system in mass/body and unsprung mass can be reduced by changing the value of the current control in the MR brake. Well in that case the system is contrrollable, because of the parameters C and α dependent of control current.

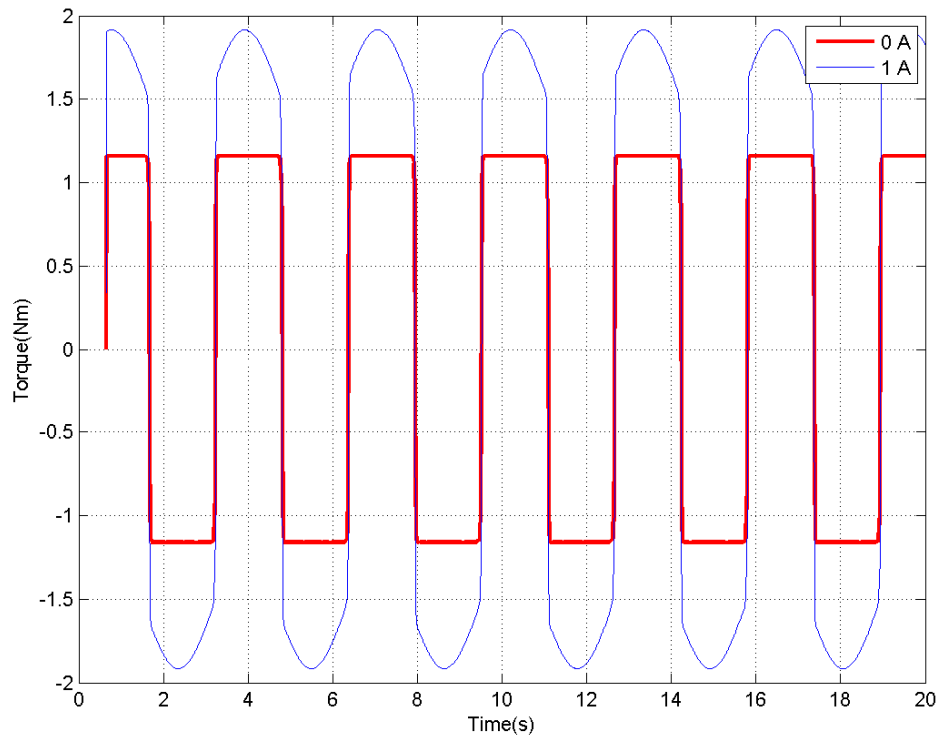


Figure 2.3.4 Simulation results in pasive and semi-active

The comparison between passive and semi- active from 0A to 1A is shown in the figure above. By increasing the current of the system, the torque increases, it means there is more damping friction in the MR brake, and body/mass of the vehicle is better stabilized.

3 Physical study

3.1 Magneto-rheological braking



Figure 3.1 MR Rotary brake

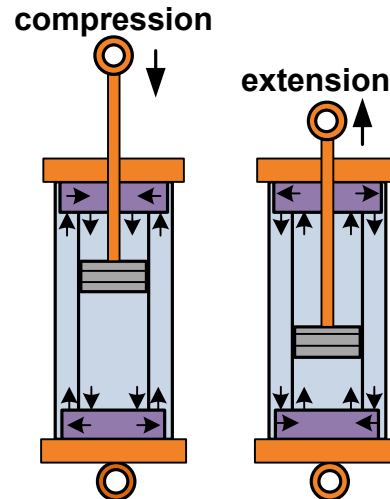


Figure 3.2 Linear MR damper

Magneto-rheological (MR) dampers are one of the semi-active control devices, which use MR fluids to provide controllable damping forces.

MR dampers are consists in two categories:

- a) Linear damper. (Right)
- b) Rotary damper. (left)

Linear damper are consists in three different dampers:

1. Monotube.
2. Twin-tube.
3. Double-ended.

The second one is rotary damper. In order to reduce vibration of the mechanical system as a kinetic and potential energy it has done built MR brake with the waveform boundary of rotary disk. The kinetic and potential energy which is generated in the mechanical system, are been saving in the MR brake, and then by re-cycling, some of the energy lost in braking into electrical energy.

Rotary brakes based on controllable fluids are passive devices with an excellent torque to weight ratio and excellent control capability.

As such, they offer a strong potential to be used in semi active suspension system like a quarter of car as well as to decrease the vibration of the car body. Higher torque to volume ratio, lower voltage and less sensitivity to impurity are the some advantages of this device.

The proposed MR brake mechanism utilizes a hybrid concept of magnetic circuit in using both axial and radial magnetic flux to generate braking force.

Magneto-rheological (MR) actuators provide controlled torque through control of an applied magnetic field. Therefore knowledge of the relationship between the applied current and output torque is required. The measured torque shows hysteresis effects as the current increases and decreases.

3.2 MR brake magnetic model



Figure 3.2. 1 MR brake structure with the form of rotary disks

In order to slow or stop a vehicle's kinetic and potential energy due to the equation of motion (Road oscillation), the MR rotary brake must be designed. In spite of this the structure of this MR brake made based on waveform boundary of rotary disk.

The aim of to design MR brake is that to investigate the hysteresis characteristics of the output torque, the input current is increased and decreased from 0A up to the max value .

In addition, the magnetic flux Φ redistributes and concentrates on the reformed MR fluid zones. The magnetic field intensity H and the magnetic flux density B increase and change their direction. The MR fluid in the MR zone is quickly to become the strong obstacles at the main working zone then the others.[1]

The distribution function of the elementary hysteresis is determined fully from the measured B-H loops.

The assumes a constitutive relation between the magnetic field H and the magnetic induction B , actually magnetic materials comprised in the electromagnetic devices have experienced demagnetization, which gives rise to a magnetic field in a direction opposite to that of the magnetization because of their open circuits. This field, called the demagnetizing field (H_d), is proportional to the intensity of magnetization (M).



Figure 3.2. 2 MR Brake Disassembled and Assembled

$$H_d = N_d M$$

Where N_d is the demagnetizing factor which depends mainly on the shape of the magnetic fluid.

The intensity of the magnetic field produced by a coil is proportional to the electric current, which follows in the coil.

$$H_a = C i$$

Where C is the coil constant, which depends on the shape of the coils and on the number of turns in the windings.

And the applied field (H_a) due to the solenoid must compensate for the demagnetizing effect to obtain a correct true field (H).

$$H = H_a - H_d$$

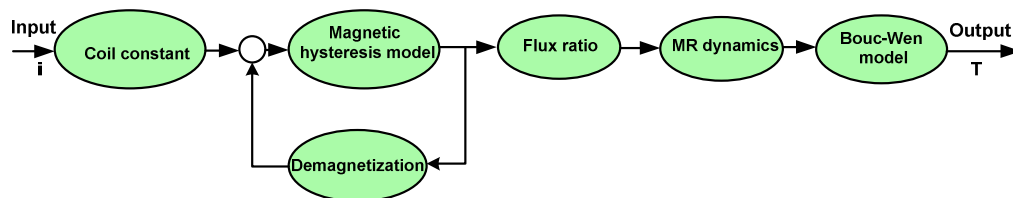


Figure 3.2. 3 Block diagram for nonlinear model of the MR brake

While the transfer function of a conventional motor can be reasonably well approximated by a constant linear relationship between input current and the output torque is shown as figure above. [2]

The geometrical of the system is shown that the how the fluid works.

Operation of MR rotary brake is based on viscosity change of MR liquid filling the chamber nr.6 between the rotor nr.3 a casing nr.7. Changing the viscosity of MR fluid is caused by current flow through the coil nr.1 which generates magnetic field nr.2. Increasing the viscosity of MR fluid increases the load torque. Then during motion of the MR brake, fluids flow through the system. [7]

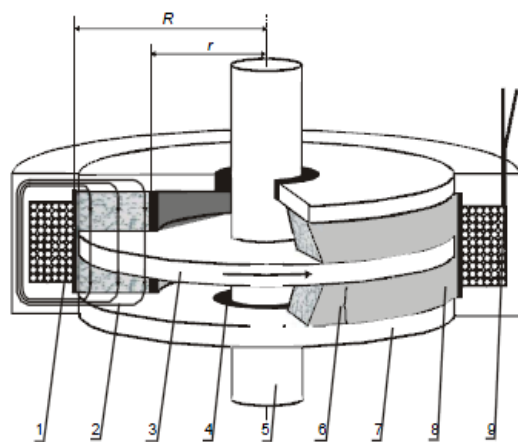


Figure 3.2. 4 Structure of MR Rotary damper

3.3 MR fluid



Figure 3.3. 1 Magnetorheological fluid

Magneto-rheological (MR) and Electro-rheological (ER) fluids are controllable fluids with varying viscosity with applied magnetic and electric fields.

MR fluids can be used in three principal modes of operation:

1. Pressure driven flow (valve) mode
2. Direct-shear mode
3. Squeeze-film mode

The valve mode is the most widely used of the three modes

In pressure driven flow (valve) mode, the two magnetic poles are fixed, and a pressurized flow of MR fluid moves between them. In direct-shear mode, the two magnetic poles move relative to each other, and the MR fluid is “sheared” between them. Squeeze-film mode involves a layer of MR fluid which is squeezed between the two magnetic poles.

MR rotary brakes can be design it with several construction. It depends on the shapes of the rotor and the geometry of the active magneto-rheological fluid.

MR brakes create braking torque by changing the viscosity of the MR fluid inside the brake. MR fluid is a type of functional fluid which has a suspension of magnetic particles in terms of carrier liquids. The particles typically with a size in order of (μm) are added to fluid, such as mineral or silicone oils. MR fluid also contains small amounts additives with effect the polarization of the particles or stabilization of the structure of the suspension to resist settling.

Operation of MR rotary damper is based on viscosity change of MR liquid filling the chamber between the rotors a casing. Changing the viscosity of MR fluid is caused by current flow through the coil which generate magnetic field. Increasing the viscosity of MR fluid increases the load torque. [1]

There are three different ways of using MR fluid, that which one of them are depend to design of MR damper where the dampers intended use. [3]

Two magnetic pole plates move relative to each other, and then shearing the Magneto-rheological fluid between them.

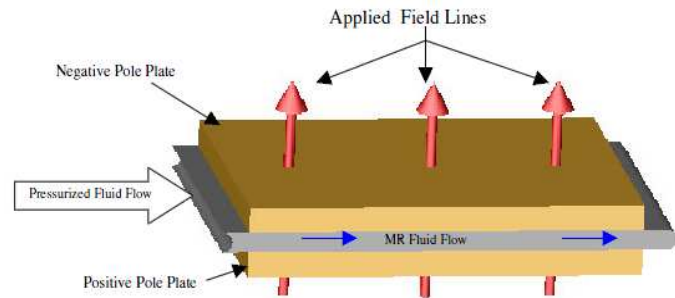


Figure 3.3. 2 MR fluid in Valve mode

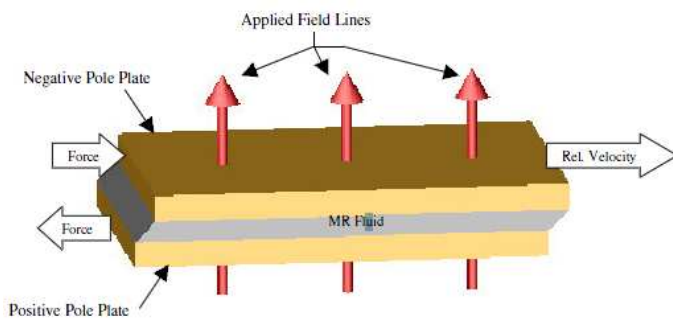


Figure 3.3. 3 MR fluid in Direct-shear Mode

The Magneto-rheological (MR) fluid is in between two paramagnetic moving surfaces. In this case the MR fluid operates in shear mode. The disadvantages of an MR fluid in shear mode are a weak connection between magnetic particles when their chains are strained by external force.

Squeeze-film mode, the third mode of MR fluid use, is used via squeezing the two magnetic pole plates together on a thin film of MR fluid
The Magneto-rheological MR fluid is in between paramagnetic pole surfaces.

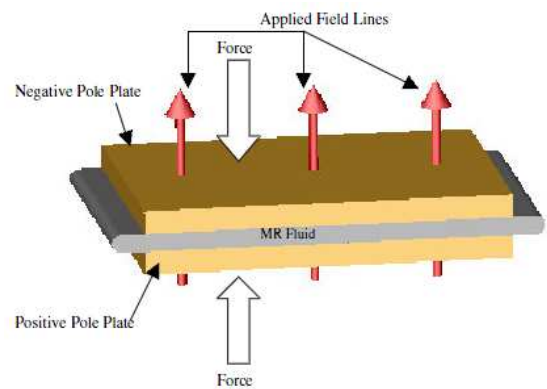


Figure 3.3. 4 MR fluid in Squeeze Mode

4 SAS system

4.1 Introduction

Physical models for the investigation of vertical dynamics of suspension systems are most commonly built on the quarter-car model.

Magneto-rheological (MR) fluids are mainly dispersion of particles made of a soft magnetic material in carrier oil. The most important advantage of these fluids over conventional mechanical interfaces is their ability to achieve a wide range of viscosity in a fraction of millisecond. This could be an efficient way to control vibrations of different device under the movement, and applications dealing with actuation, damping, robotics and mechatronics.

However, by use of dynamic mathematical model simulation, it is possible to analyze the behavior and performance of systems consisting of rigid or flexible parts undergoing displacement motions.

4.1.1 Purpose

Vibration control of vehicle suspensions (quarter of car) systems has been an active subject of research, since it can provide a good performance for drivers and passengers. Recently, many researchers have investigated the application of MR fluids in the controllable dampers for semi-active suspensions; it means control with the current. This work has the purpose of characterizing, identifying the mathematical model and simulating the behavior of a MR fluid in car suspension systems.

4.1.2 System description

The MR device designed in this research is a rotational damper through which an electro-magnet rotates MR fluid. The semi-active suspension system consists of a rocking lever that emulates the quarter of car body, whereas a spring and an MR damper simulate the semiactive vibration control.

A DC motor coupled to an eccentric wheel due to the same shaft is used to simulate the vibrations induced to the vehicle. A set of equations that model the dynamics of the suspension system are given in this chapter, in which the detailed definitions of the angles and distances are provided.

4.2 Components

4.2.1 Encoder

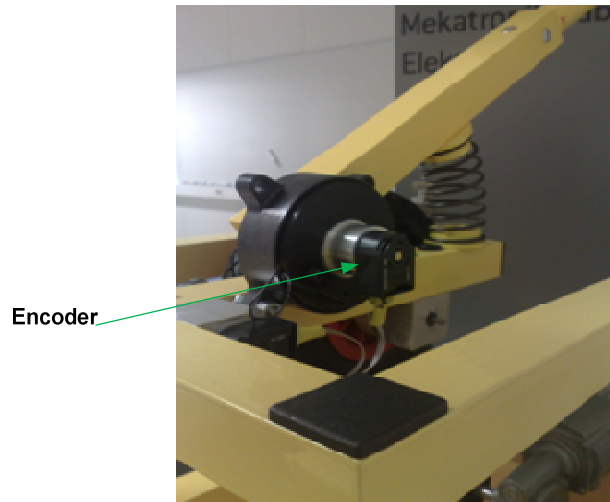


Figure 4.2. 1 Encoder of the experimental setup behind of MR brake

An encoder is a device, transducer or software program and algorithm that convert information from one format, or code to another.

Encoders have become the most popular device for measuring angular speed and position within a motor drive or at the shaft of a wheel or steering mechanism to provide a high-resolution output of the motor position and hence give an accurate measurement of the arm position via MR brake to the computers program. (See figure 4.2 1)[10]

In the SAS mechanical system, encoders are placed at the end of rotational axis of upper beam, shaft connecting DC motor with cam and lower beam. The first one is selected to measure rotation of the upper beam. The second gives feedback about the angular position of the eccentric wheel (excitation measurement). The last one informs about the rotation of the lower beam.

Therefore, the encoder which is installed behind of MR brake is calculating the angle $(\alpha_1 - \alpha_2)$, the angle of body/mass in relation to horizontal line. The difference of those two angles is the one angle, which is called (θ) .

$$\theta = \alpha_1 - \alpha_2 \quad \text{Also} \quad \dot{\theta} = \left(\frac{d\alpha_1}{dt} - \frac{d\alpha_2}{dt} \right)$$

The encoders output a continuous signal covering a range of 4096 pulses from the arm moving from one end stop to the other. The encoders send the signals to a data, and this data is stored in shared memory through a compiled Simulink file.

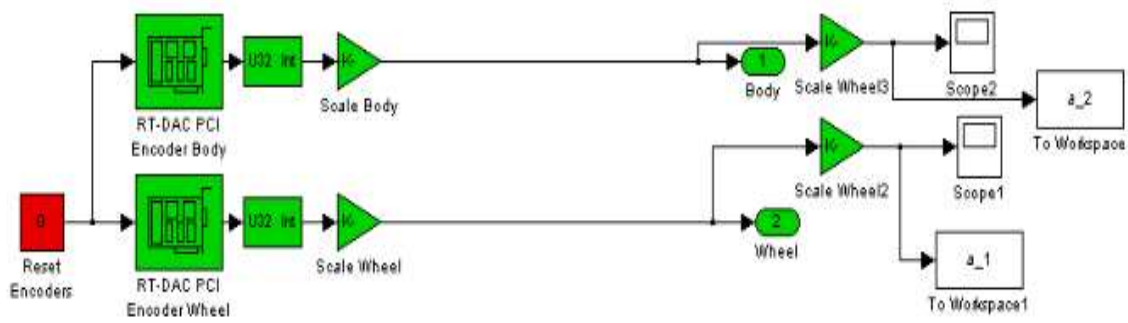


Figure 4.2. 2 Simulink block diagram of encoder in experimental setup

This model tell that, the measuring of the angle between the body and and unsprung mass in the two difference angle in relation to horizontal line. Here it is measurements of the pulses in each encoder.

$$\text{Sensitivity (pulses per degree)} = \frac{\text{Output over given Range (pulses)}}{\text{Size of Range (Degree)}} = \frac{4096}{360} = 11$$

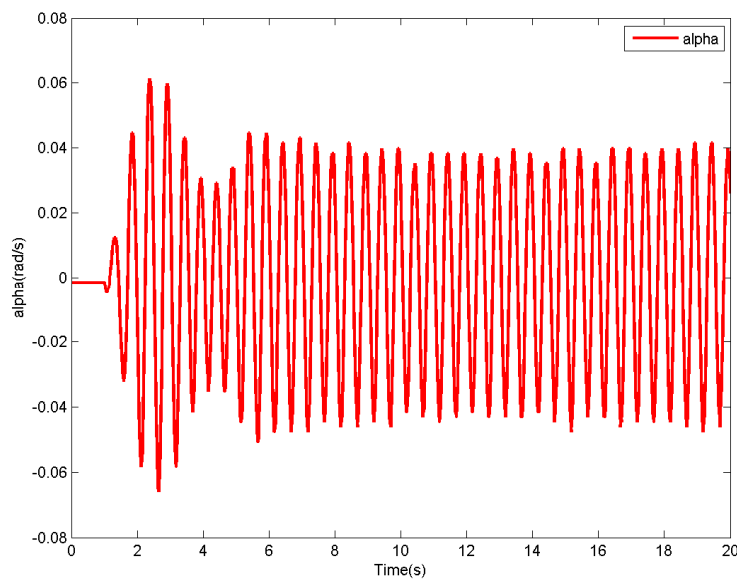


Figure 4.2. 3 Encoders Simulink result

The simulink result of encoder in (rad/s), of the MR brake in the 20s, which shows the difference between two angles. (α_1, α_2)

4.2.2 Body

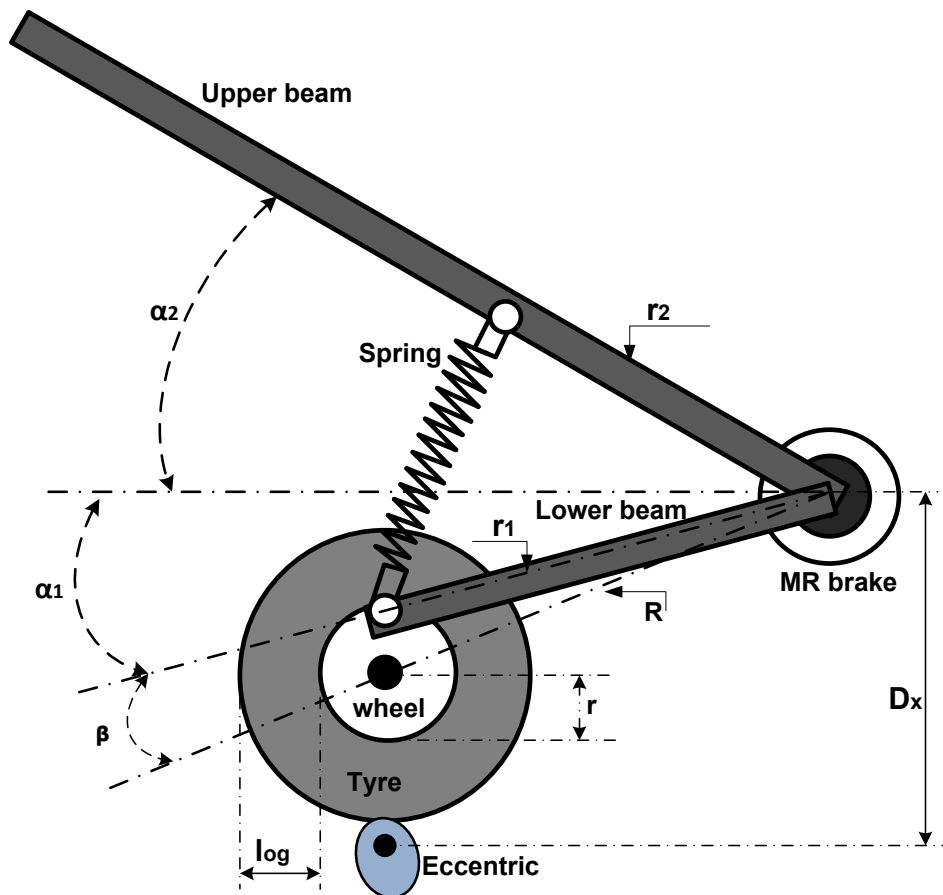


Figure 4.2. 4 Geometrical diagram of semi active system

In the mechanical picture, that is shown in the figure 4.2 4. there are two main equation of torque which is coming in to MR brake. The first one is, the torque equation of the upper beam, and the second one is the torque equation of the lower beam, which is the lower beam is connected to the wheel, then the wheel is like a follower of eccentric, which there is a equation of motion is driven by eccentricity.

In this section the mechanical equations are explained in the simple part, and then the dynamic model of semi active suspension system of those two important part is described by the following differential equations during the project.

4.2.3 Body calculation geometry

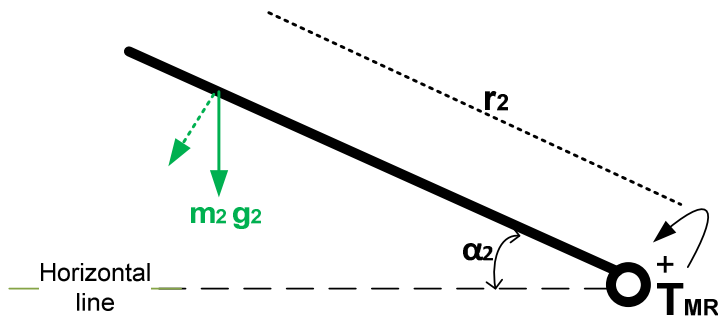


Figure 4.2.5 Body Geometry

G_2 : it is the gravitational forces torque of the body, which is the Newton second law. Mass of upper beam is multiplied by gravitational. Potential energy of the mass of body.

$$G_2 = m_2 g_2 \quad (\text{N})$$

$$m_2 g_2 r_2 \cos\alpha_2 = M_{T_{MR}} \quad (\text{Nm})$$

4.2.4 Spring calculation

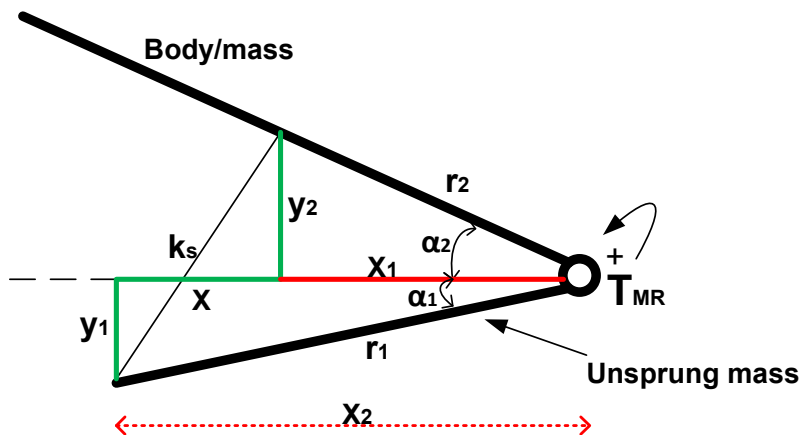


Figure 4.2.6 Spring Geometry

The spring equation is describe in below:

$$T = r_2 k_s \left(l_{0s} - \sqrt{(r_2 \cos\alpha_2 - r_1 \cos\alpha_1)^2 + (r_2 \sin\alpha_2 - r_1 \sin\alpha_1)^2} \right)$$

When the system is in running, then the linear spring is in elongation, then the force of the spring make the moment of inertia in to the MR brake.

Pythagorean theorem

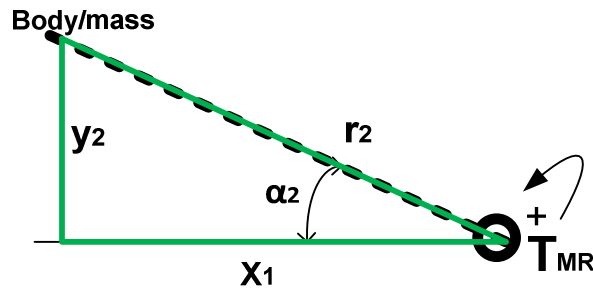


Figure 4.2. 7 Pythagorean calculation of spring due to the body

$$\sin\alpha_2 = \frac{y_2}{r_2}, \quad y_2 = r_2 \sin\alpha_2$$

$$\cos\alpha_2 = \frac{x_1}{r_2}, \quad x_1 = r_2 \cos\alpha_2$$

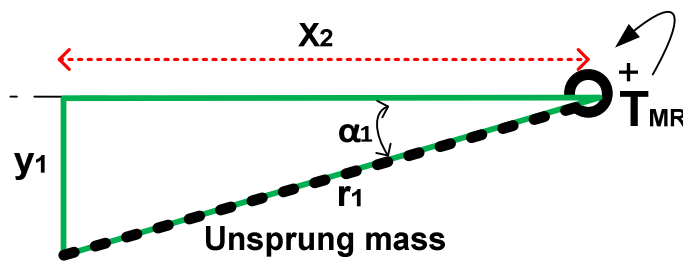


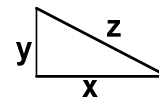
Figure 4.2. 8 Pythagorean calculation of spring due to the unsprung mass

$$\sin\alpha_1 = \frac{y_1}{r_1}, \quad y_1 = r_1 \sin\alpha_1$$

$$\cos\alpha_1 = \frac{x_2}{r_1}, \quad x_2 = r_1 \cos\alpha_1$$

$$z^2 = x^2 + y^2$$

$$z^2 = x^2 + y^2$$



The calculation of the spring in the details is described above, in both direction of the spring movement.

The figure 4.2. 7 explain calculation of spring due to the body, and the figure 4.2. 8 explain calculation of spring due to the unsprung mass.

Spring stiffness equation: this equation (4.2.4), explain the force in the spring, which is the spring in extension and reduction between the upper beam and lower beam. In another case the equation of spring is in elongation and compress. Then the equation explain the moment of spring in relation to the MR brake.

Mathematically by using Hooke's law states that is possible to calculate the elastic potential energy (spring force).

According to the Hooke's law equation

Then:

$$F = -k (x - x_0)$$

$$F = -k_s (l_{os} - l_o)$$

The loaded spring between upper beam and lower beam:

$$l_o = \sqrt{(r_2 \cos \alpha_2 - r_1 \cos \alpha_1)^2 + (r_2 \sin \alpha_2 - r_1 \sin \alpha_1)^2}$$

And then :

$$F_s = k_s (l_{os} - \sqrt{(r_2 \cos \alpha_2 - r_1 \cos \alpha_1)^2 + (r_2 \sin \alpha_2 - r_1 \sin \alpha_1)^2})$$

Torque equation for spring:

$$T = -arm k_s (l_{os} - l_o)$$

$$T_{MR} = r_2 k_s (l_{os} - \sqrt{(r_2 \cos \alpha_2 - r_1 \cos \alpha_1)^2 + (r_2 \sin \alpha_2 - r_1 \sin \alpha_1)^2}) \quad (4.2.4)$$

Where:

- α_2 : is the angle between the upper beam and horizontal line.
- α_1 : is the angle between the lower beam and horizontal line.
- r_1, r_2 : are the distances between the spring mount and the beam (the lower and upper beam).
- k_s : is the elasticity coefficient of the spring.
- l_{os} : is the length of the no load spring.
- l_o : is the length of the loaded spring between upper beam and lower beam.

4.2.5 Tire elasticity

T_{sT} is the actuating kinematic torque which is transferred through the tire.

Based on the Hook's second law:

$$F = -k_g x \quad (\text{N})$$

$$F = -k_g (l_{og} + R \sin(\beta - \alpha_1) + r - D_x + u_{kin})$$

Torque of tire elasticity: $T = -arm k_g (x)$

Where the:

$(l_{og} + R \sin(\beta - \alpha_1) + r - D_x + u_{kin})$ is the displacement of elasticity of the tire between the input of Eccentricity (u_{kin}), and the tire absorption, or the displacement between excitation and tire.

k_g is the elasticity coefficient of the tire in the unit (Nm^{-1} or $kg s^{-2}$).

Torque of tire elasticity: $T = -arm k_g (x) \quad (\text{Nm})$

$$T_{sT} = -k_g R \cos(\beta - \alpha_1) (l_{og} + R \sin(\beta - \alpha_1) + r - D_x + u_{kin}) \quad (\text{Nm})$$

The elasticity coefficient of the tire in to the MR brake by connecting with lower beam.

The elasticity coefficient of the tire is called (k_g) which is coming force of the tire in to the center of the wheel.

Then there is a compression from the tire in to the lower beam in connection point to push the unsprung mass (lower beam) up, and the same compression of the spring, which is push the unsprung mass down. This compression in the tire is called (l_{og}). In another case l_{og} is the length of the loded spring of the tire. (See figure4.3. 1).

4.2.6 Linear movement calculation

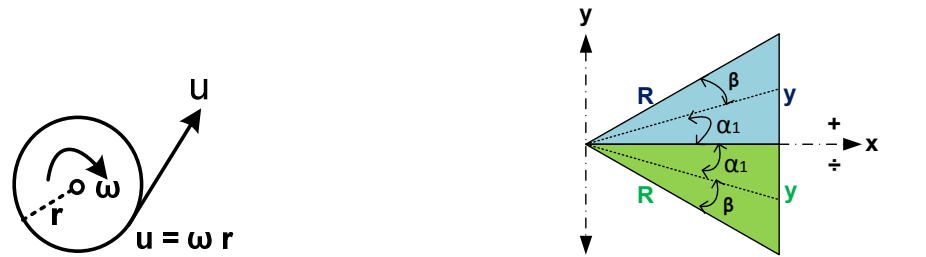


Figure 4.2. 9 Linear movement calculation

$$y = R \sin (\beta + \alpha_1)$$

$$y = R \sin (\beta - \alpha_1)$$

The figure above explain the linear movement of the wheel, which is moving in vertical direction, when the eccentric is running, therefore the wheel has both rotational speed and linear movement.

T_{DT} is the damping torque generated by the tire gum, when the tire gum hits the U_{kin} then create the lump or compression, in another case it is the absorption coefficient of the tire. See figure 4.3. 2

$$T_{DT} = f_g \dot{x}$$

Where the:

\dot{x} : is the derivation of the displacement of tire elasticity. $\left(\frac{m}{s}\right)$

f_g : is the damping coefficient. $\left(\frac{Ns}{m}\right)$

$$T_{DT} = f_g \left(\frac{d(D_x - U_{kin})}{dt} - \omega r \right) \quad (Nm)$$

Then the kinetic torque energy is:

$$T_{DT} = -f_g \left(\frac{d(D_x - u_{kin})}{dt} - \frac{d\alpha_1}{dt} R \cos(\beta - \alpha_1) \right)$$

This equation explain the torque of the tire, when the tire hits the road. In this case the road oscillation is shown by the eccentric wich is connected to motor. See figure 4.3. 6. The U_{kin} is the input of sinusoidal.

The whole equation tells about the moment from the tire in the point that have a connection with the eccentric in to the MR brake.

$$\begin{aligned}
& J_1 \frac{d^2 \alpha_1}{dt^2} - k_1 \frac{d\alpha_1}{dt} + m_1 g_1 r_1 \cos(\beta - \alpha_1) + \\
& + r_1 k_s (l_{0s} - \sqrt{(r_2 \cos \alpha_2 - r_1 \cos \alpha_1)^2 + (r_2 \sin \alpha_2 - r_1 \sin \alpha_1)^2}) \\
& - k_g R \cos(\beta - \alpha_1) (l_{0g} + R \sin(\beta - \alpha_1) + r - D_x + u_{kin}) \\
& - f_g \left(\frac{d(D_x - u_{kin})}{dt} - \frac{d\alpha_1}{dt} R \cos(\beta - \alpha_1) \right) = \left(\frac{d\alpha_1}{dt} - \frac{d\alpha_2}{dt} \right) M_{MR}(i)
\end{aligned}$$

The equation above explain the torque of the lower beam, which is most interesting for the control system of the semi-active-suspension system. Well in that case there are two forces, that is going to the end of the unsprung mass/ lower beam. First is the equation of the motion, which is coming from eccentric through the follower (wheel), and the second is the force from the spring, which is connected to the upper beam/ body. Where the u_{kin} is the input of sinusoidal.

$$T_{unsprung\ mass} = J_1 \frac{d^2 \alpha_1}{dt^2} \quad (4.3.1)$$

$$T_{viscous} = -k_1 \frac{d\alpha_1}{dt} \quad (4.3.2)$$

$$T_{G\ lower} = m_1 g_1 r_1 \cos(\beta - \alpha_1) \quad (4.3.3)$$

$$T_{spring} = r_1 k_s (l_{0s} - \sqrt{(r_2 \cos \alpha_2 - r_1 \cos \alpha_1)^2 + (r_2 \sin \alpha_2 - r_1 \sin \alpha_1)^2}) \quad (4.3.4)$$

$$T_{ST} = -k_g R \cos(\beta - \alpha_1) (l_{0g} + R \sin(\beta - \alpha_1) + r - D_x + u_{kin}) \quad (4.3.5)$$

$$T_{DT} = -f_g \left(\frac{d(D_x - u_{kin})}{dt} - \frac{d\alpha_1}{dt} R \cos(\beta - \alpha_1) \right) \quad (4.3.6)$$

The $T_{unsprung\ mass}$ is the moment of inertia of lower beam or unsprung mass, which is the potential energy of the lower body.

$T_{viscous}$ is the viscous friction damping torque, that is that is kinematic energy of the MR brake, when it is in rotational.

$T_{G\ lower}$ the torque is the potential energy of the lower beam.

T_{spring} the spring torque which is the kinetic energy of the spring.

T_{ST} the elasticity spring torque of tire which has the potential energy, because of elasticity of the tire.

T_{DT} the damping torque of the, when there is a connection between tire and Eccentric. Then there is potential energy, if there is not any connection between tire and eccentric, and there is a kinetic energy if there is a connection between them, the energy is generated by motor.

4.3 Geometry Torque Representation

4.3.1 Upper beam Analysis

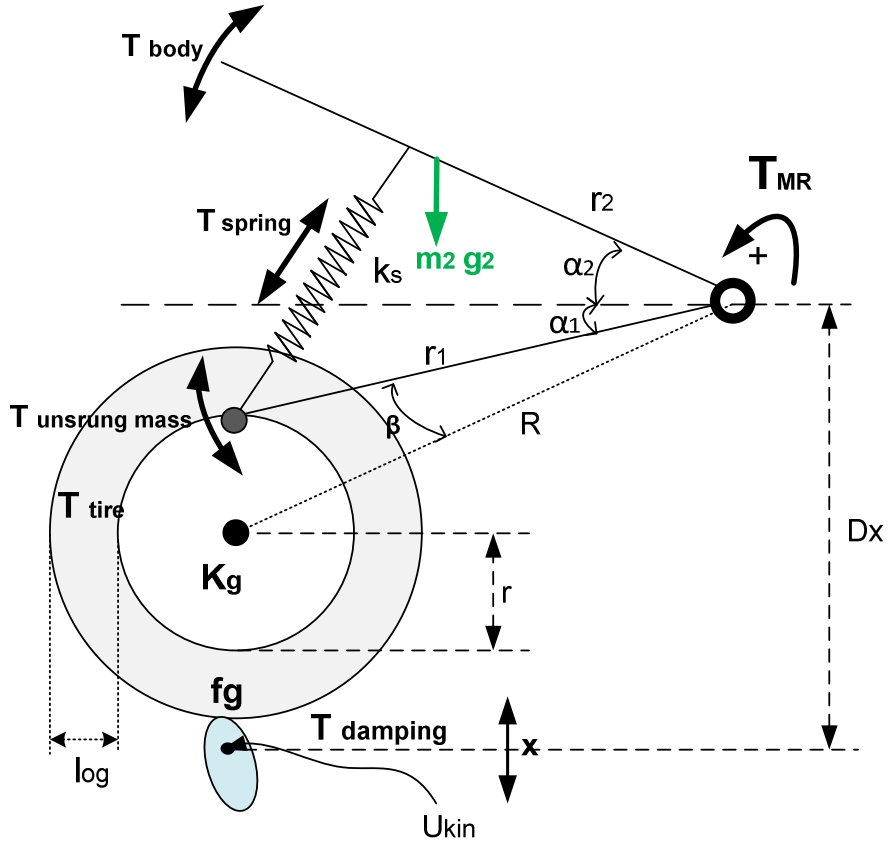


Figure 4.3. 1 Upper beam analysis

Torque for upper beam/body

Based on the Newton second law:

$$\sum T_{sum} = J \dot{\omega}$$

$$T_{body} + T_{G\ upper} - T_{spring} - T_{viscous} = T_{MR}$$

$$J_2 \dot{\omega}_2 + m_2 g r_2 \cos\alpha_2 - r_2 F_s - k_2 \omega_2 = c \omega$$

$$J_2 \ddot{\alpha}_2 + m_2 g r_2 \cos\alpha_2 - r_2 k_s (l_{os} - l_0) - k_2 \dot{\alpha}_2 = c \dot{\alpha}$$

$$J_2 \ddot{\alpha}_2 + m_2 g r_2 \cos\alpha_2 - r_2 k_s (l_{os} - \sqrt{lx^2 + ly^2}) - k_2 \dot{\alpha}_2 = c \dot{\alpha}$$

$$J_2 \ddot{\alpha}_2 + m_2 g r_2 \cos\alpha_2 - r_2 k_s \left(l_{os} - \sqrt{(r_2 \cos\alpha_2 - r_1 \cos\alpha_1)^2 + (r_2 \sin\alpha_2 - r_1 \sin\alpha_1)^2} \right) - k_2 \dot{\alpha}_2 = c (\dot{\alpha}_1 - \dot{\alpha}_2)$$

$$T_{body} = J_2 \frac{d^2 \alpha_2}{dt^2} \quad (4.2.1)$$

$$T_{viscous} = k_2 \frac{d\alpha_2}{dt} \quad (4.2.2)$$

$$T_G = m_2 g r_2 \cos \alpha_2 \quad (4.2.3)$$

$$T_{spring} = r_2 k_s \left(l_{0s} - \sqrt{(r_2 \cos \alpha_2 - r_1 \cos \alpha_1)^2 + (r_2 \sin \alpha_2 - r_1 \sin \alpha_1)^2} \right) \quad (4.2.4)$$

And finally the torque for upper beam in to the MR brake is:

$$J_2 \frac{d^2 \alpha_2}{dt^2} - k_2 \frac{d\alpha_2}{dt} + m_2 g r_2 \cos \alpha_2 - r_2 k_s \left(l_{0s} - \sqrt{(r_2 \cos \alpha_2 - r_1 \cos \alpha_1)^2 + (r_2 \sin \alpha_2 - r_1 \sin \alpha_1)^2} \right) = \left(\frac{d\alpha_1}{dt} - \frac{d\alpha_2}{dt} \right) M_{MR}(i)$$

Where:

T_{body} : The moment of inertia of the upper beam due to the Mr brake. J_2 is multipleid by the angular accelaration. The equation commes from the Newtom second low.

J_2 : is the moment of inertia of the upper beam with respect to its axis of roation.

$T_{viscous}$: The viscous moment of the upper beam in to MR brake. there is a viscous moment in the magnetor-heological brake.

k_2 : is the viscous friction coefficient of the upper beam.

T_G : is the gravitational force torque.

T_{spring} : it is the moment of the spring in to the MR brake.

4.3.2 Lower beam Analysis

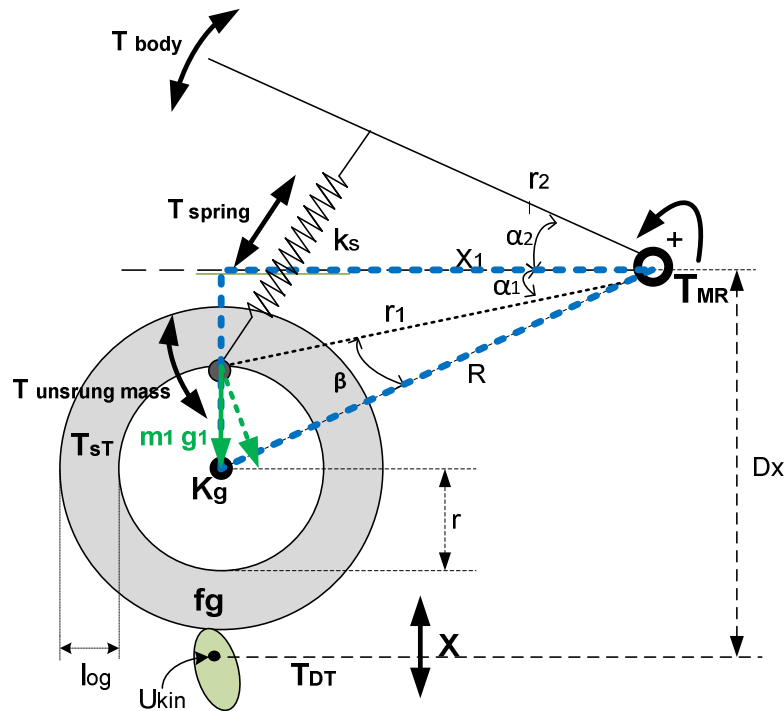


Figure 4.3.2 Gravitational moment of lowerbeam

The G_1 is the gravitational moment of the lower beam, which is include the mass and gravitation with the angle of lower beam in to horisontal line. Potential energy of the unsprung mass.

$$G_1 = m_1 g_1 \quad (N)$$

$$m_1 g_1 r_1 \cos (\beta - \alpha_1) = M_{T_{MR}} \quad (Nm)$$

Moment of spring in to the MR brake, which is obtained of the spring stiffness equation is the same equation like as upper beam analysis but the lower beam is arm (r_1) for this equation. See eq. below

$$T_{MR} = r_1 k_s \left(l_{0s} - \sqrt{(r_2 \cos \alpha_2 - r_1 \cos \alpha_1)^2 + (r_2 \sin \alpha_2 - r_1 \sin \alpha_1)^2} \right)$$

Based on the Newton second law there is:

$$\sum T_{sum} = J \dot{\omega}$$

$$T_{unsprung\ mass} + T_{G\ lower} - T_{spring} - T_{viscous} - T_{sT} - T_{DT} = T_{MR}$$

$$J_1 \dot{\omega}_1 + m_1 g r_1 \cos(\beta - \alpha_1) - r_1 F_s - k_1 \omega_1 - F_{sT} r - f_g \dot{x} = c \omega$$

$$J_1 \ddot{\alpha}_1 + m_1 g r_1 \cos(\beta - \alpha_1) - r_1 k_s (l_{os} - l_0) - k_1 \dot{\alpha}_1 - k_g x r - f_g (\dot{x}_{Ecc} - \dot{x}_{lowerbeam}) = c \dot{\alpha}$$

Where the 'c' is the damping in the MR brake.

$$J_1 \ddot{\alpha}_1 + m_1 g r_1 \cos(\beta - \alpha_1) - r_1 k_s (l_{os} - \sqrt{lx^2 + ly^2}) - k_1 \dot{\alpha}_1 - k_g R \cos(\beta - \alpha_1) (l_{og} + R \sin(\beta - \alpha_1) + r - D_x + u_{kin}) - f_g \left(\frac{d(D_x - U_{kin})}{dt} - \omega r \right) = c \dot{\alpha}$$

$$J_1 \ddot{\alpha}_1 + m_1 g r_1 \cos(\beta - \alpha_1) - r_1 k_s \left(l_{os} - \sqrt{(r_2 \cos \alpha_2 - r_1 \cos \alpha_1)^2 + (r_2 \sin \alpha_2 - r_1 \sin \alpha_1)^2} \right) - k_1 \dot{\alpha}_1 - k_g R \cos(\beta - \alpha_1) (l_{og} + R \sin(\beta - \alpha_1) + r - D_x + u_{kin}) - f_g \left(\frac{d(D_x - U_{kin})}{dt} - \dot{\alpha}_1 R \sin(\beta - \alpha_1) \right) = c (\dot{\alpha}_1 - \dot{\alpha}_1)$$

$$J_1 \frac{d^2 \alpha_1}{dt^2} - k_1 \frac{d\alpha_1}{dt} + m_1 g_1 r_1 \cos(\beta - \alpha_1) + r_1 k_s (l_{os} - \sqrt{(r_2 \cos \alpha_2 - r_1 \cos \alpha_1)^2 + (r_2 \sin \alpha_2 - r_1 \sin \alpha_1)^2} - k_g R \cos(\beta - \alpha_1) (l_{og} + R \sin(\beta - \alpha_1) + r - D_x + u_{kin}) - f_g \left(\frac{d(D_x - u_{kin})}{dt} - \frac{d\alpha_1}{dt} R \cos(\beta - \alpha_1) \right) = \left(\frac{d\alpha_1}{dt} - \frac{d\alpha_2}{dt} \right) M_{MR(i)}$$

Where:

J_1 : is the moment of inertia of the lower beam/unsprung mass with respect to its axis rotation.

k_1 : is the viscous friction coefficient of the lower beam.

r : is the radius of the wheel rim.

l_{0s} : is the length of the no-load spring between upper beam and lower beam.

l_{0g} : is the length of the loaded spring of the tire.

l_0 : is the length of the loaded spring between upper beam and lower beam.

k_s : is the elasticity coefficient of the spring.

f_g : is the absorption coefficient of the tire.

i : is the current of the rotary MR brake.

u_{kin} : Is the kinetic sinusoidal excitation.

D_x : is the distance between the beam pivot and the pivot of the eccentric.

β : is the angle between lower beam and the horizontal line.

k_1 : is the viscous friction coefficient of the lower beam.

T_{sT} : the kinematic actuating torque transferred through the tire.

$M_{MR(i)}$: is the static profile of the MR brake.

$m_1 g$: is the gravitational moment of the lower beam.

$m_2 g$: is the gravitational moment of the upper beam.

4.4 Real experimental data

There are two ways to find the torque in Magneto-rheological brake (MR brake). The first one is direct torque measurement by a transducer .

Another way to find the torque is to use the dynamic equations of motion of the mechanical setup. The system which is analysed in this work can simulate a car suspension system – it means a quarter of car body.

According of the explanation the dynamic equation in section 4.3

The torque equation of the upper beam is given by:

$$T_{body} + T_{G\ upper} - T_{spring} - T_{viscous} = T_{MR}(i)$$

Therefore the torque equation due to the spring can be written as:

$$T_{spring} = -T_{body} - T_{G\ upper} + T_{viscous} + T_{MR}$$

Then:

$$T_{spring} = - \frac{J_2 \alpha_2 - m_2 g \ddot{r}_2 \cos\alpha_2 + k_2 \dot{\alpha}_2 + c \dot{\alpha}}{r_2 k_s}$$

Since the torque generated by the spring is present in equations of motion of both: upper and lower beams, it is possible to connect those two formulas together. It is done by expressing torque generated in the spring in terms of the equation of motion of the upper beam and substituting it to the equation of motion of the lower beam, which is given by the formula:

$$T_{unsprung\ mass} + T_{G\ lower} - T_{spring} - T_{viscous} - T_{sT} - T_{DT} = T_{MR}(i)$$

By following the steps described above finally it is obtained :

$$T_{unsprung\ mass} + T_{G\ lower} - \frac{J_2 \alpha_2 - m_2 g \ddot{r}_2 \cos\alpha_2 + k_2 \dot{\alpha}_2 + c \dot{\alpha}}{r_2 k_s} - T_{viscous} - T_{sT} - T_{DT} = T_{MR}(i)$$

Since those two dynamic equations are connected now, it is possible to calculate the torque generated in the Magneto-rheological damper.

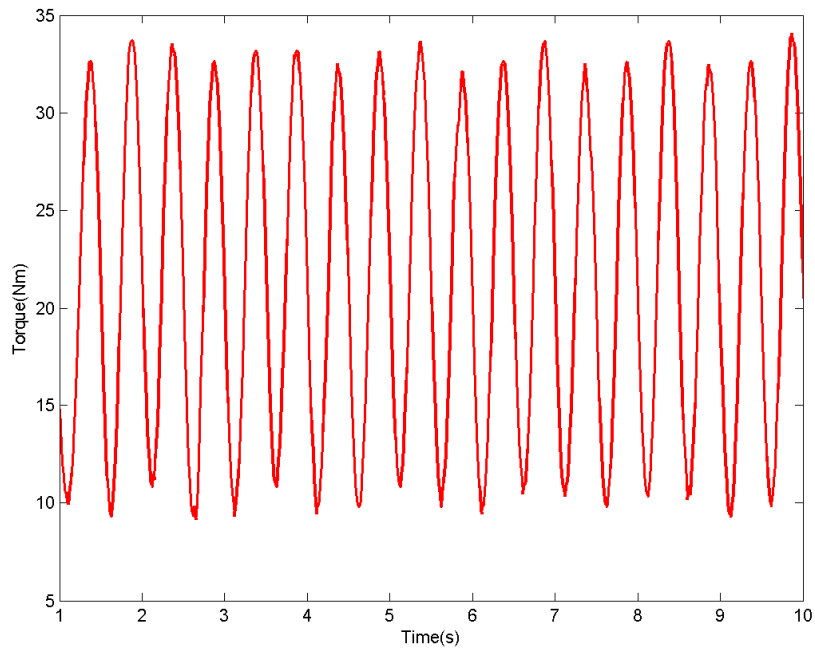


Figure 4.4.1 Simulation result of real experimental data

The figure above shows the torque simulating dynamic equation from real experimental data. It illustrates generation of the hysteresis in the MR brake, because the amplitude from the top point to the middle of the graph, and from bottom to the middle of the graph is not equal.

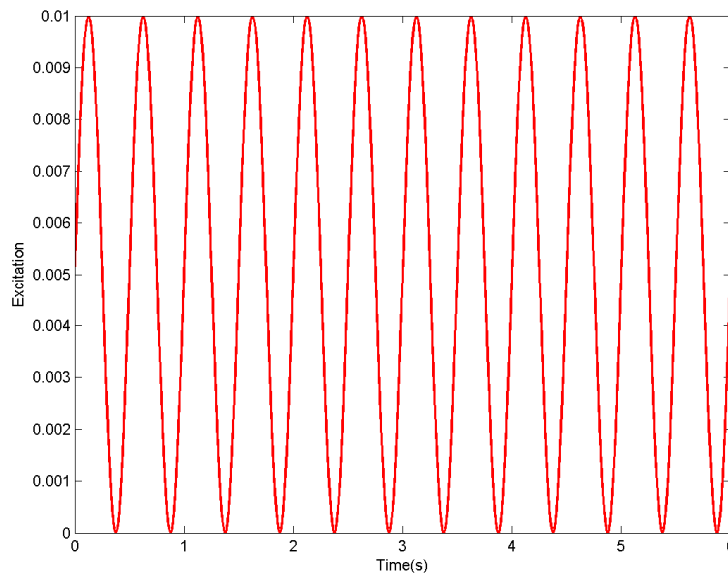
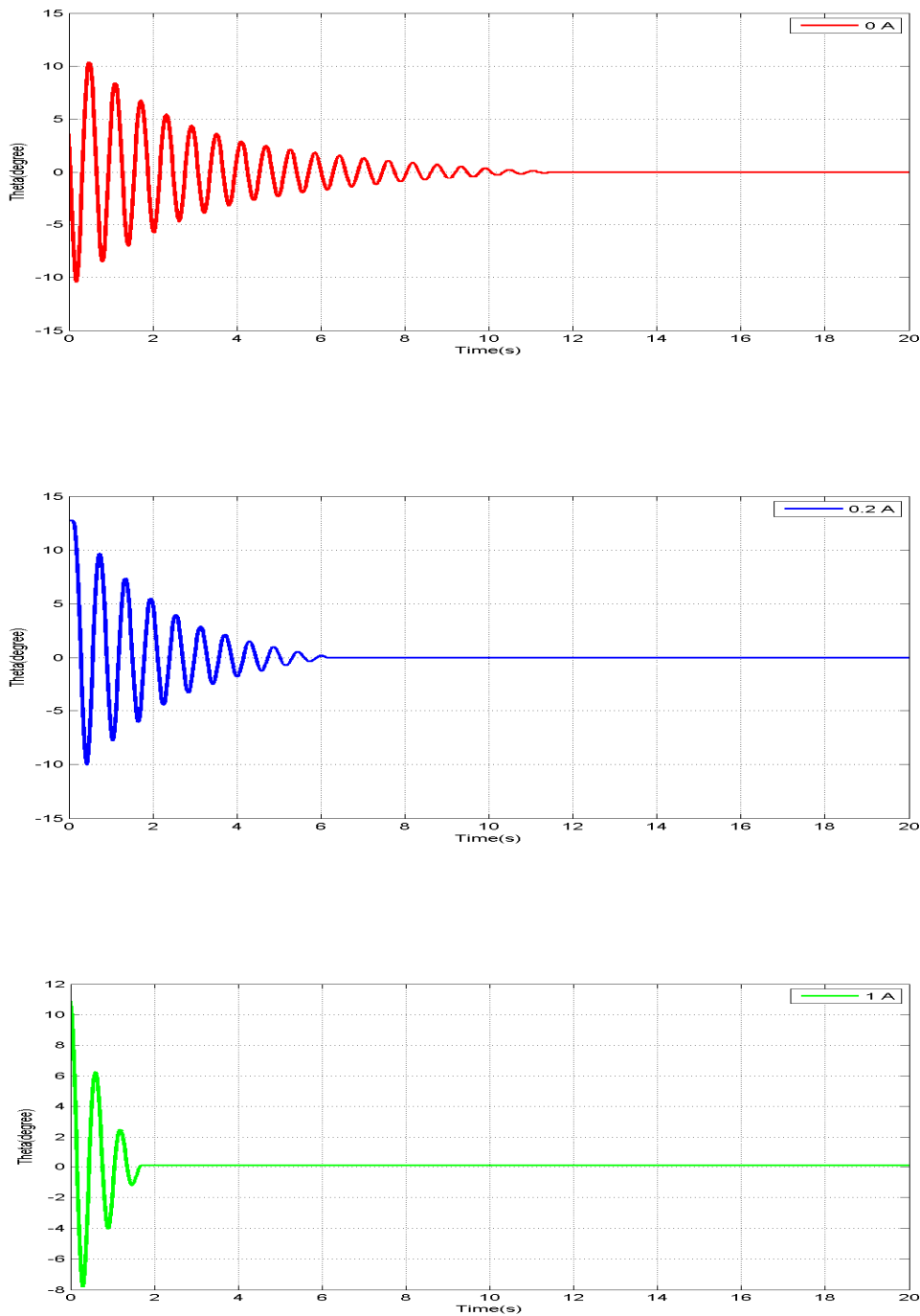


Figure 4.4.2 Excitation input

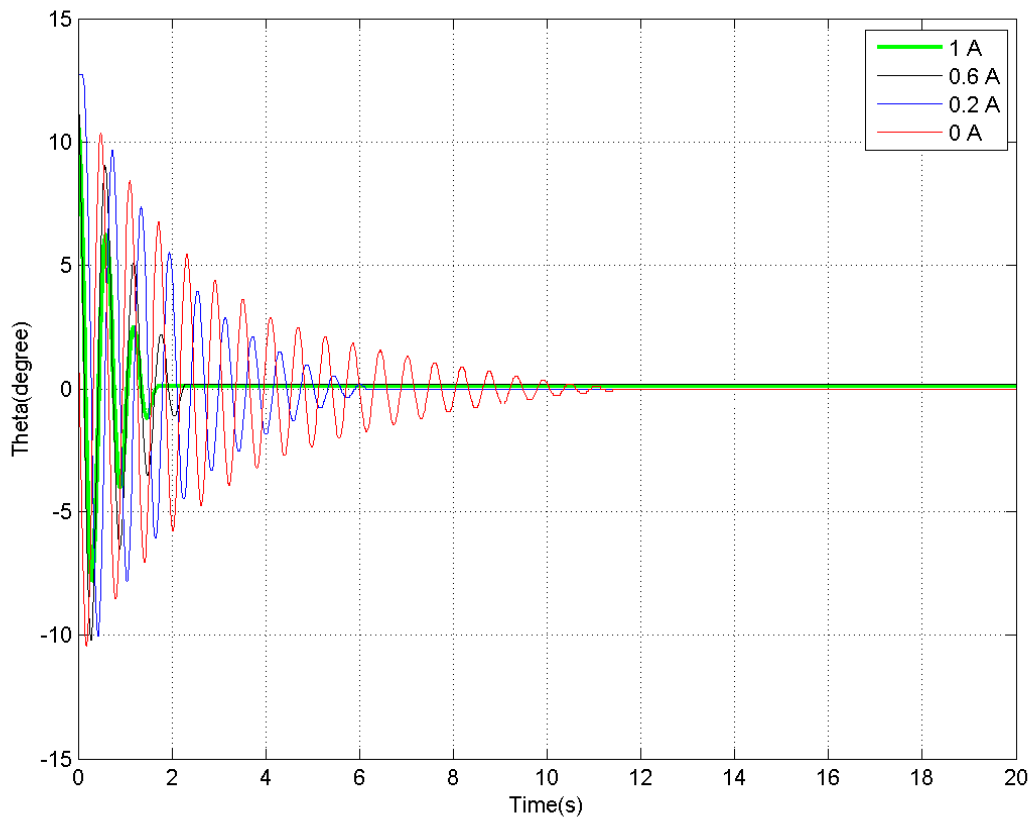
The excitation in the simulink program is sine wave - see figure above.

4.4.1 Experimental Damping



Figur 4.4.3 Damping coefficient of MR brake

Three pictures above illustrate responses of the system for changable input – current ranging from 0A to 1A. the angle theta which is angular displacement of the upper beam has been measured by the encoder.



Figur 4.4.4 Damping simulation of MR brake

The different control current input from 0A to 1A shows that the vibration of the body is reduced.

For the 0 Amper the bodies vibration goes to the stable in around 11 seconds, and by changing the current from 0A to the 0.2A as a input the system is going to stable in 6 seconds. In another case by increasing the control input of current, the damper friction in the Magneto-rheological (MR) rotary brake fluid is increasing. And also the vibration of the body is going to stabilize in the shorter time.

5 Identification

5.1 Parameters Estimation

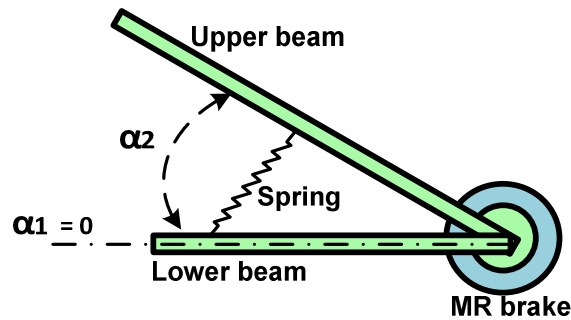


Figure 5.1. 1 Estimation method

An important part of this research is to describe dynamic equation of the system. Measurements of the angular position of the upper beam were made by releasing it manually from a random angle ($\alpha_2 = 16^\circ$) and then running the system without rotation of the wheel. See the figure 5.1.1. According to the torque equation for the upper beam/body that is explained in chapter 4.3.1 there is:

$$T_{Gravity} - T_{spring} - T_{viscous} - T_{MR} = J \dot{\omega}$$

Where:

$$T_{body} : J_2 \frac{d^2\alpha_2}{dt^2} \quad (4.2.1)$$

$$T_{viscous} : k_2 \frac{d\alpha_2}{dt} \quad (4.2.2)$$

$$T_{Gravity} : m_2 g r_2 \cos\alpha_2 \quad (4.2.3)$$

$$T_{spring} : r_2 k_s \left(l_{0s} - \sqrt{(r_2 \cos\alpha_2 - r_1 \cos\alpha_1)^2 + (r_2 \sin\alpha_2 - r_1 \sin\alpha_1)^2} \right) \quad (4.2.4)$$

$$T_{MR} : c \dot{\omega} + \alpha z$$

Those equations above describe the torque from the upper beam due to the Magnetorheological damper. In this way the T_{MR} is the function of input to the simulink block diagram, to estimating the mathematical model such as Bouc-Wen, Dahl and Bingham models.

These equations are implemented in MATLAB/SIMULINK for evaluating its performance.

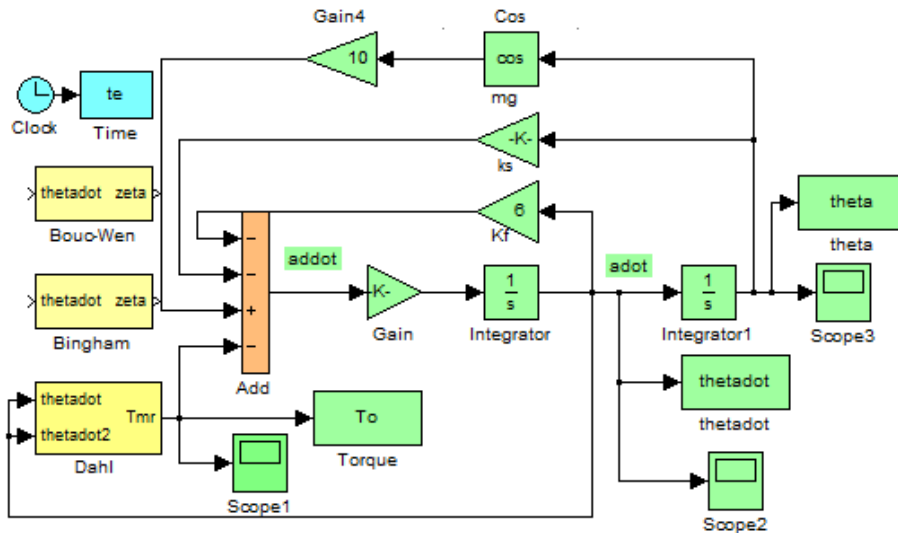


Figure 5.1. 2 Simulink dynamic model

Comparison of the models

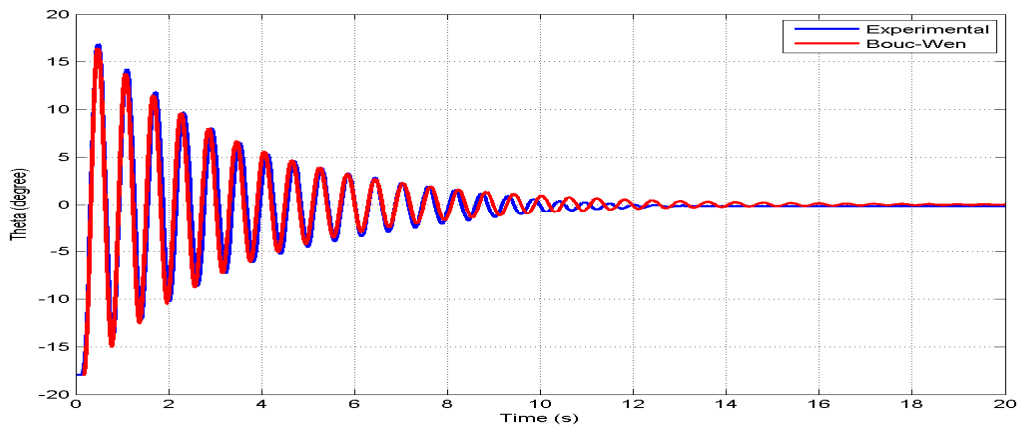


Figure 5.1.3 Bouc-Wen model approximation

The graph above illustrates the fitting procedure of the output of equation presented in Figure 5.1.2 to the experimental measurements. This was done in the trial-and-error method in order to determine parameters characterizing Bouc-Wen model.

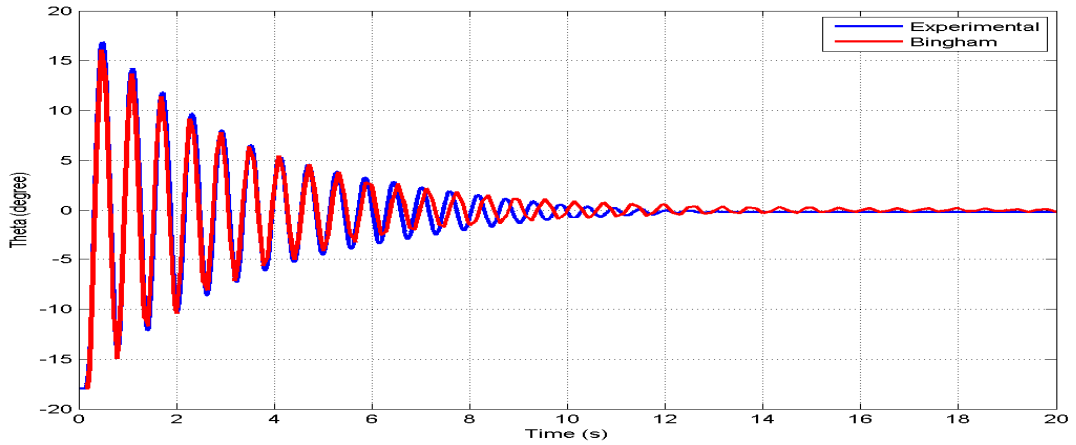


Figure 5.1.4 Bingham model approximation

The parameters estimation of the Bingham model is not as precise as Bouc-Wen model estimation. The figure above shows that the system after 12 second has some oscillation, while the experimental setup is stable after 12 sec.

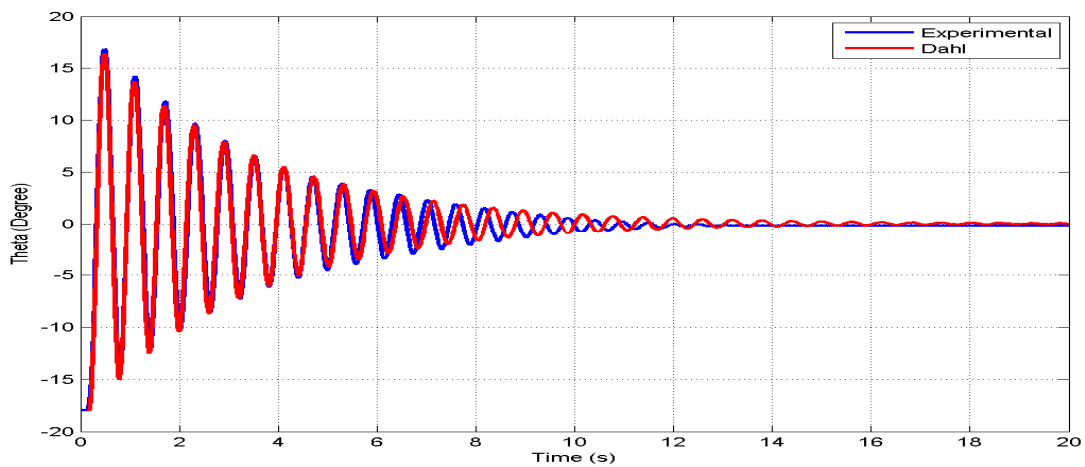


Figure 5.1.5 Dahl model approximation

By comparing those three different mathematical models by using the expeimental graph(blue) in the last three figures, it is concluded that the Bouc-Wen model gives the best estimation for the hysteretic characteristic.

Bouc-Wen model

Several mathematical models have been proposed to describe the hysteretic behavior of systems. The aim of this chapter (5), is that to estimate the parameters of different mathematical model, and then identify the parameters by using the the function of torque. Eq.1

The Bouc-Wen model is one of the solutions, which is used more for hysteretic nonlinearities, and the model can capture many commonly observed types of hysteretic behavior. This nonlinear differential equation model reflects local history dependence through introducing an extra state variable. [9]

The physical model of the MR damper is the torque due to the Bouc-Wen model element given by (see eq.1 eq.2). Where the damping coefficient C , and α are linearly which is dependent of the current (i).

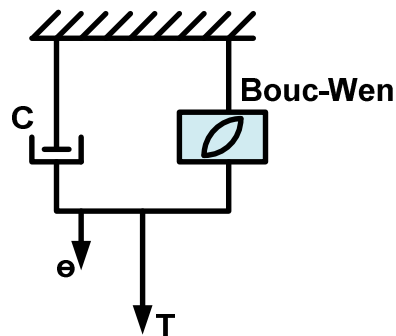
The set of initial conditions $z(0)$ for which the signal $z(t)$ is bounded for every piecewise continuous signal $\dot{\theta}$. The following analysis determines the set as an explicit function of the Bouc-Wen model parameters.

$$T_{MR} = \alpha(i)z + C(i)\dot{\theta} \quad (1)$$

$$\dot{z} = -\gamma|\dot{\theta}|z|z|^n - \beta\dot{\theta}|z|^n + \delta\dot{\theta} \quad (2)$$

$$C(i) = C_0 + C_1(i)$$

$$\alpha(i) = \alpha_0 + \alpha_1(i)$$



Figur 5.1.6 Bouc-Wen Model of the MR Damper

The parameters γ, β, δ and also n of Bouc-Wen model is uncertain and non dimensional parameters which control the shape and the size of hysteresis graph.

Where:

- | | |
|------------------------------------|--|
| C | Is the sign of rotational damper (damping coefficient). |
| T | Is the Torque. |
| $\alpha, \beta, \gamma, n, \delta$ | Are model parameters have to be identified. |
| Z | The z is an evolutionary variable that describes the hysteresis. |
| \dot{Z} | Denotes the time derivate. |
| $\dot{\theta}$ | Is the rotational damping velocity (MR brake angular velocity). |

5.1.1.1 Parameters Analysis

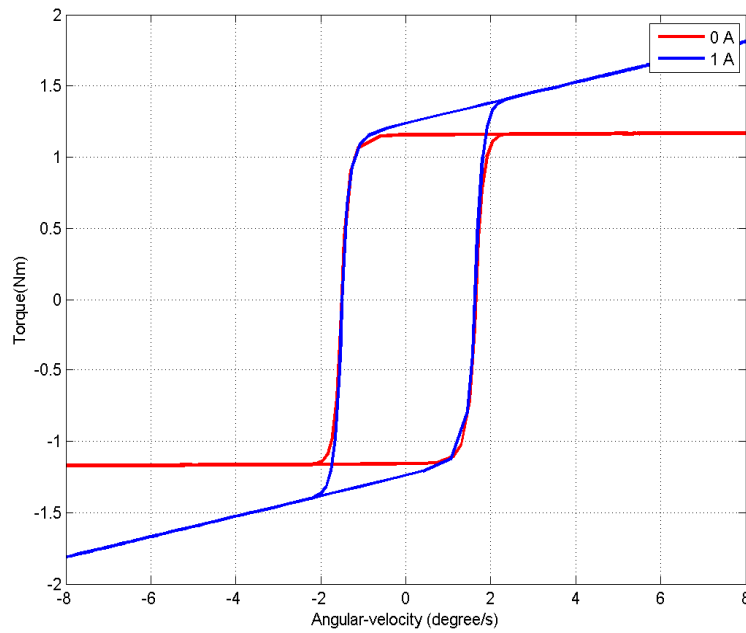
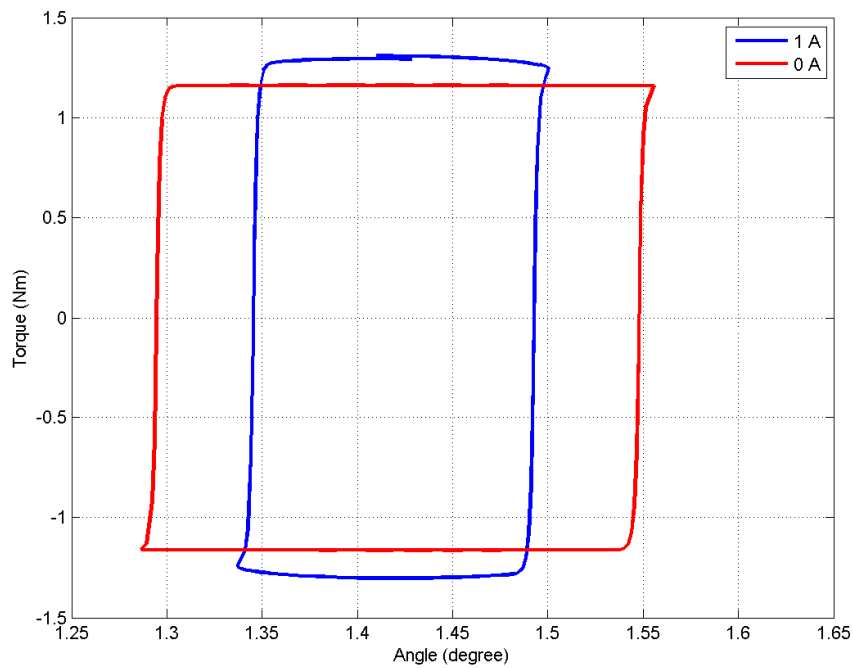


Figure 5.1. 7 Dynamic characteristic Torque-Angular velocity

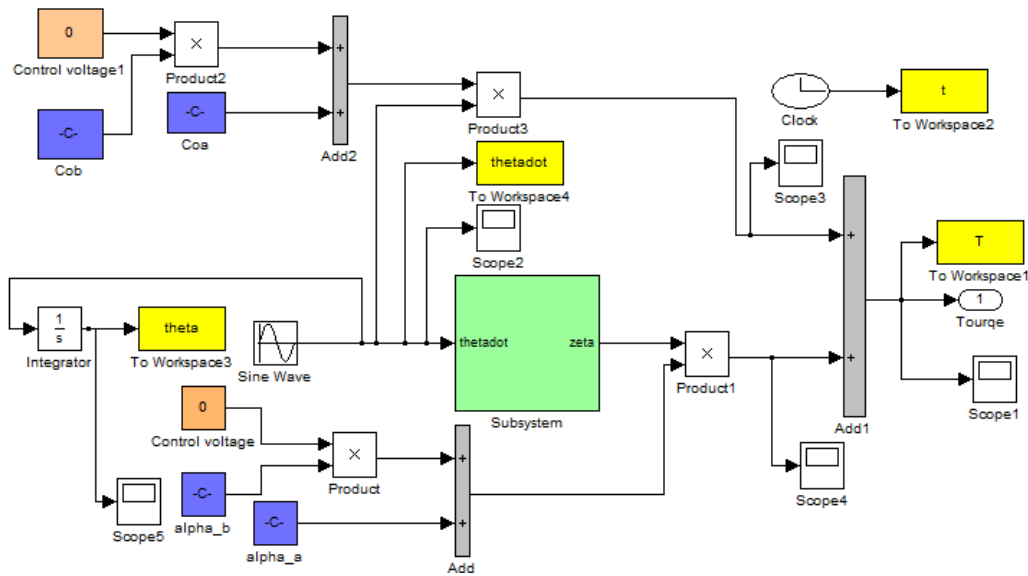
For current equals to 0A, the system is pasive. For 1A is semi active.



Figur 5.1. 8 Dynamic characteristic Torque-Angle

The simulation results of the Bouc-Wen model which are shown in the figures above prove that the model gives the acceptable estimation of parameters for the hysteretic characteristic.

Simulink diagram of Bouc-Wen model



Figur 5.1. 9 Simulink block diagram of Bouc-Wen model.

In the simulink model above the sin wave has been used as angular velocity. The parameter α and damping coefficient C are current dependent.

Parameters Identification

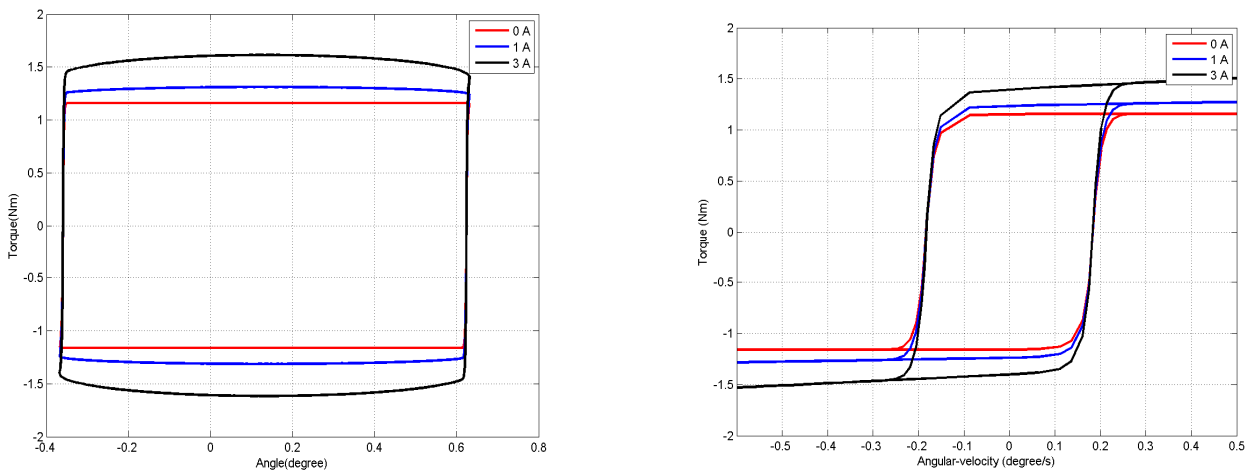


Figure 5.1. 10 Identification Torque-Angular velocity and Torque-Angle

The experimental observation shows that torque and velocity hysteresis are coming closer to zero torque value by changing the input current (i) from 0A up to the 3A. Look at figures above.

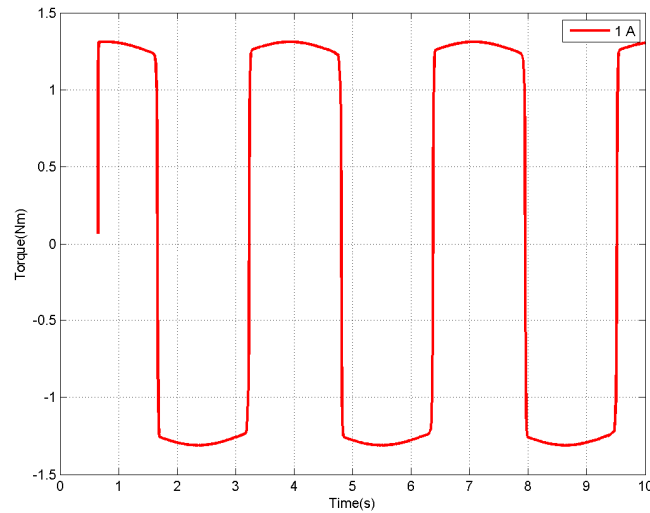


Figure 5.1.12 Torque-Time

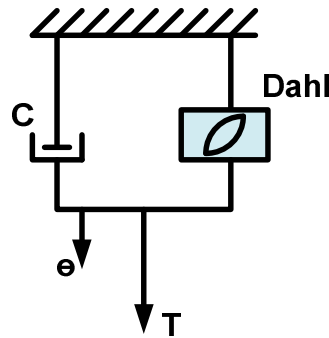
Simulation results confirm that the higher current is applied, the higher torque is generated, resulting in increasing system's damping. Bouc-Wen model parameters listed in the table below were determined in the parameter identification stage of this work.

Parameters	Value	Unit
β	737	
γ	1	
δ	843	
N	0,9	
Coa	0,0015	Ns/m
Cob	0,07	Ns/m
α_a	1	N/m
α_b	0,07	N/m

Table 3 Bouc-Wen model parameters

The simulation results in figures 5.1 10 and 5.1 12 shows that the parameters estimation is acceptable, and those parameters above capture the hysteresis loop.

5.1.2 Dahl model



Figur 5.2. 1 Dahl mechanical model

$$T_{MR} = k_x(i) \dot{\theta}(t) + k_w(i) z(t) \quad 5.1$$

$$\dot{z} = \rho (\dot{\theta} - |\dot{\theta}| z) \quad 5.2$$

$$k_x = k_{x_a} + k_{x_b}(i)$$

$$k_w = k_{w_a} + k_{w_b}(i)$$

Dahl model can also use for the experimental setup to test the MR brake for hysteresis behavior.

The Dahl model is the Coulomb friction element in the change of friction of the force, when the direction of motion is changed. The model is established of viscous and Dahl which is shown in figure above. The mathematical model is in the eq. (5.1-5.2).

Where k_x and k_w is the current dependent.

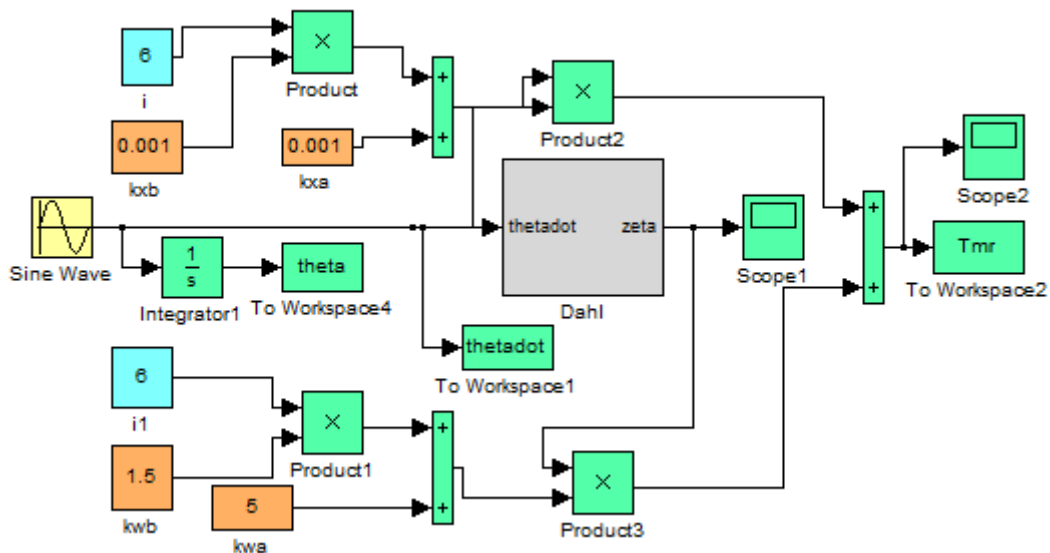


Figure 5.2. 2 Simulink diagram of function of torque due to the MR brake

5.1.2.1 Parameters Analysis

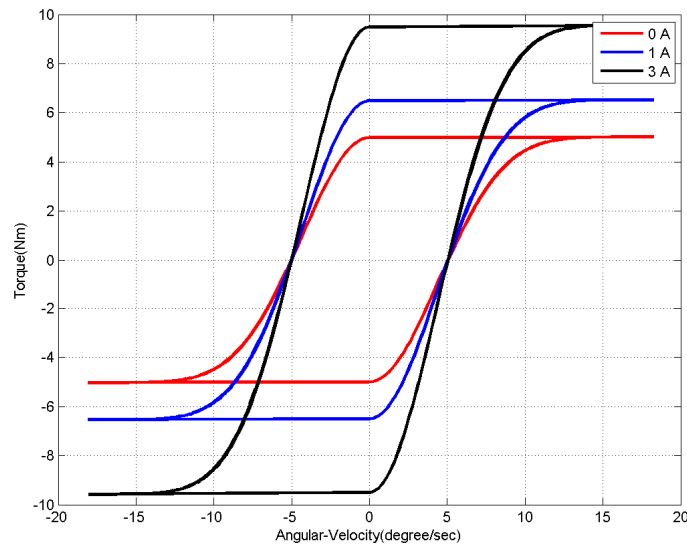


Figure 5.2. 3 Torque - Angular velocity (deg/sec)

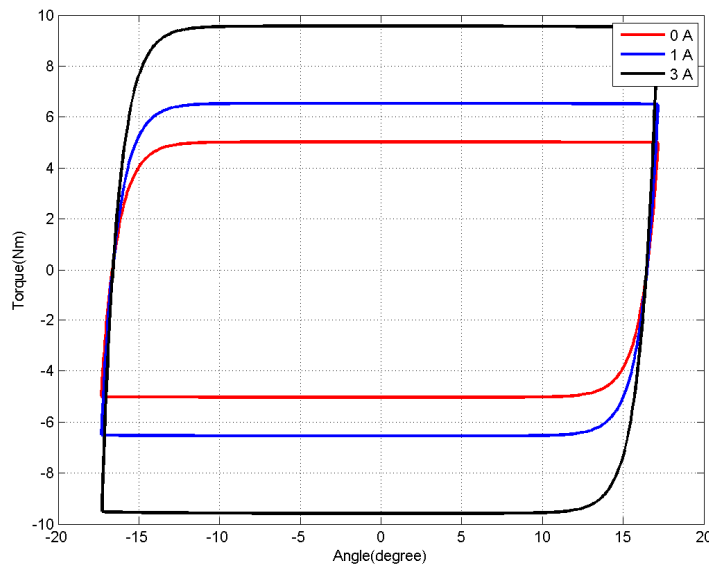
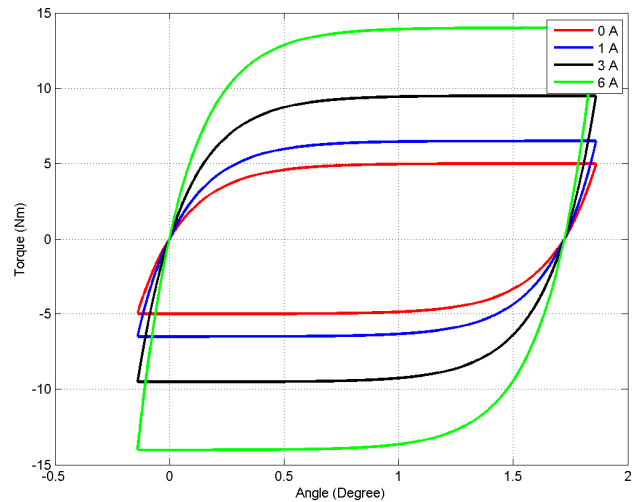
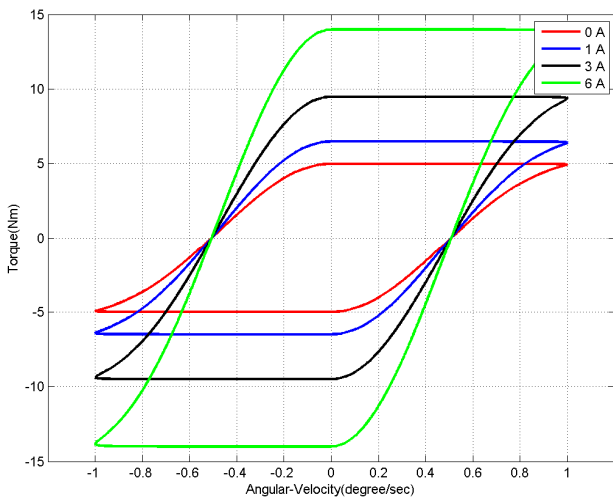


Figure 5.2. 4 Torque - Angle(deg)

By fitting the displacement curve to the experimental curve from bodies angle in figure (5.1.3), it has been generated those hysteresis graphs in the different input current (A), from 0A up to 3A (Amp). The hysteresis loop of the parameters explain that the estimation of parameters are acceptable. In the next page the parameters are tested in the function of torque of Magneto-rheological (MR) rotary brake.

5.1.2.2 Parametrs Identification



Parameters	Value	Unit
kxa	0,001	Ns/m
kxb	0,001	Ns/m
ρ	5	
kwa	5	N/m
kwb	1,5	N/m

Table 4 Dahl model parameters

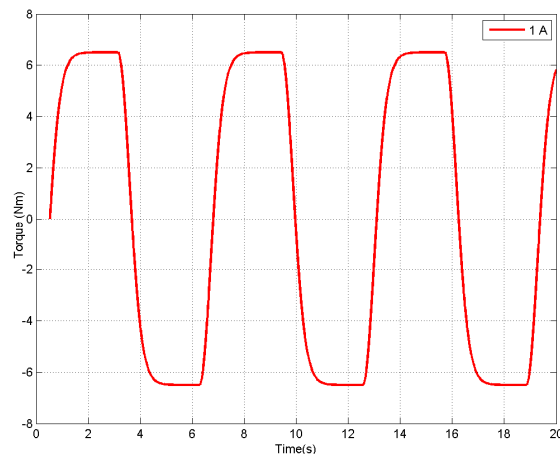
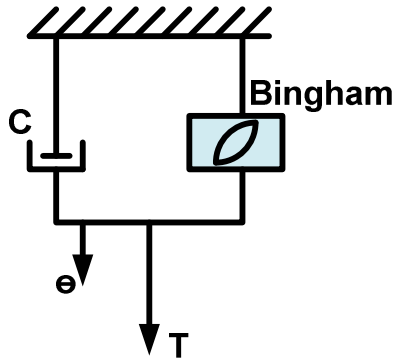


Figure 5.2. 5 Simulation result parameters of Dahl model

The simulation results of the Dahl parameters show that the identification of parameters is correct. The hysteresis loop of Torque- Angular velocity is increasing from 0A up to the 6A. By increasing the current, the Magneto-rheological (MR) brake generate more torque, and rotational speed of the MR brake decreases. Also, in hysteresis loop of the Torque-Angle it is visible that the displacement of the angle is reduced, and finally the vibration of the body goes to the stable state.

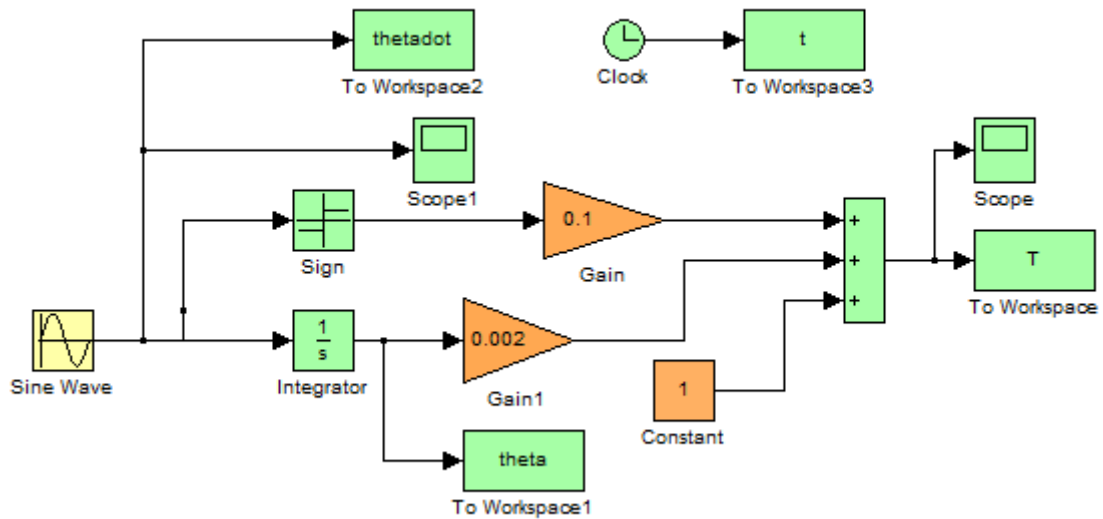
5.1.3 Bingham model



Figur 5.3. 1 Bingham Model of a Controllable Fluid

$$T_{mr} = f_c * sgn(\dot{\theta}) + c_0\theta + f_0 \quad 5.3$$

The Bingham model has been used to characterize MR and ER fluids. The model consists of a Coulomb friction element placed in parallel with a viscous damper, which is shown in figure above. In this model the torque generated by the device given by eq. (5.3), where c_0 is the damping coefficient and f_c is the friction force, f_0 is non zero, it means observed in the measured force due to the presence of the accumulator.



Figur 5.3.2 Simulink diagram of Bingham

5.1.3.1 Parameters Analysis

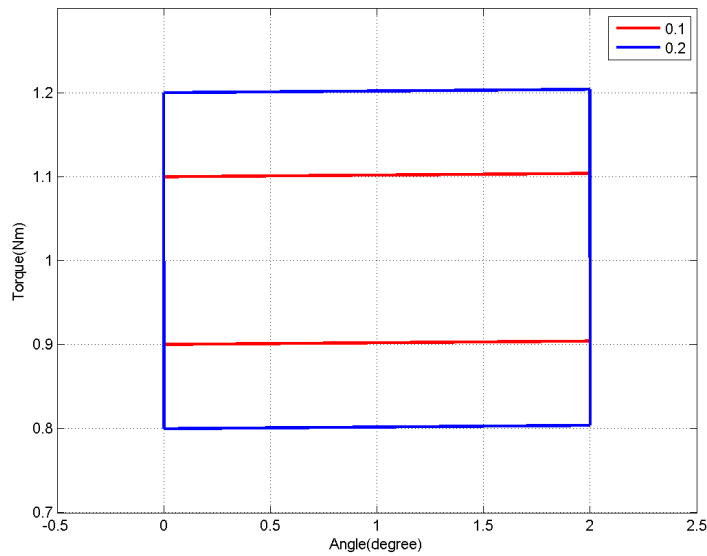


Figure 5.3. 3 Torque - Angle (Deg)

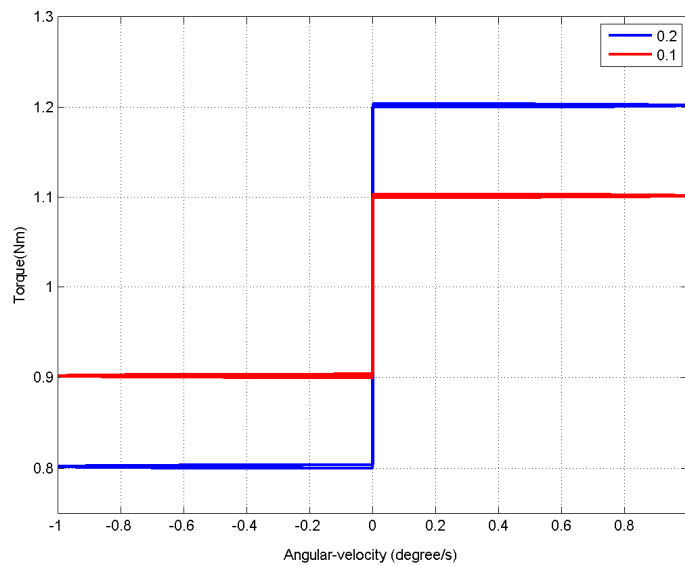
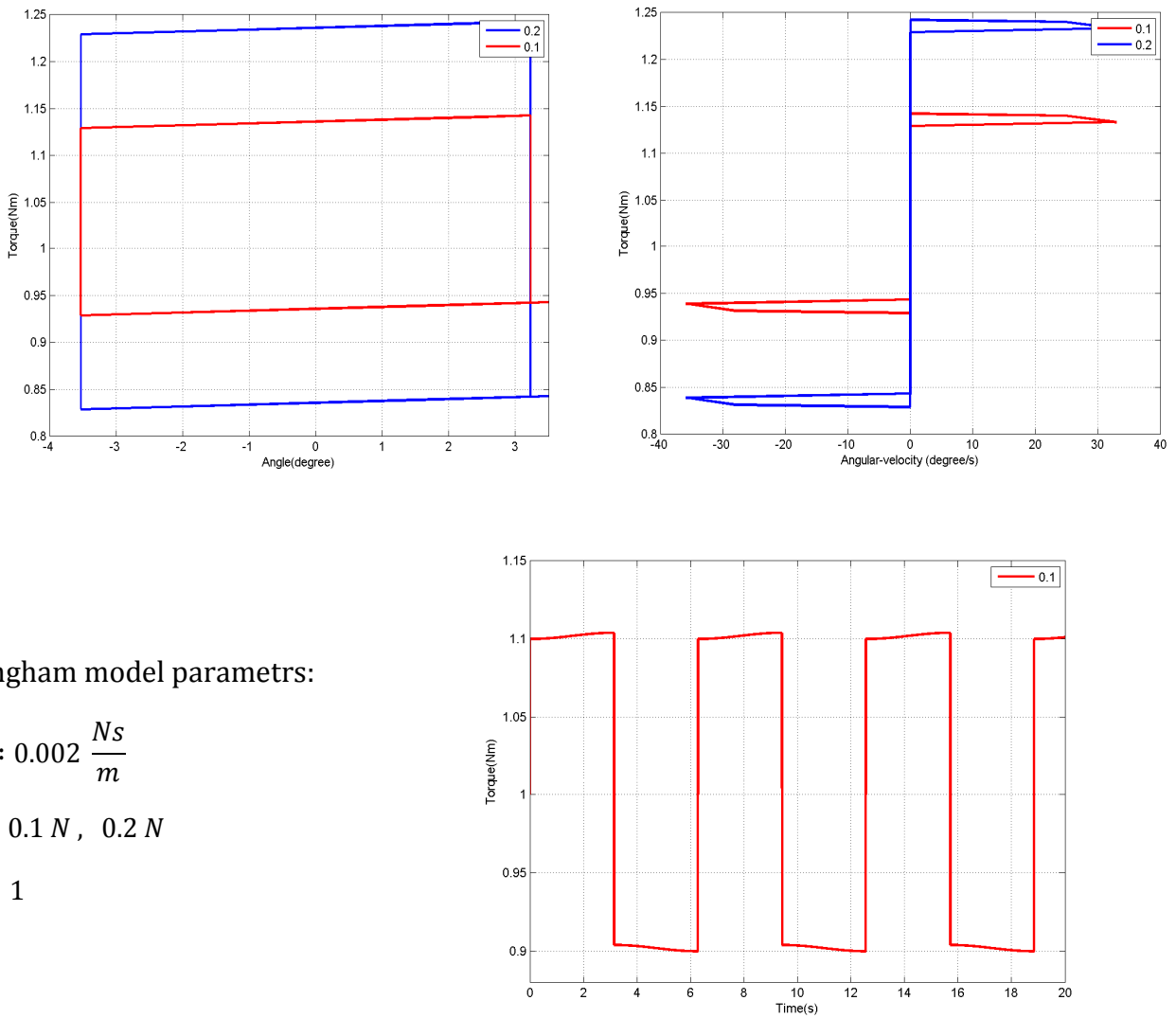


Figure 5.3. 4 Torque - Angular velocity (Deg/sec)

The estimation parameters for the Bingham mathematical model is also produced the hystersis loop, but the difference is that the Bingham model parameters do not capture the hysteresis loop as Bouc-Wen and Dahl models do.

5.1.3.2 Parameters Identification



Bingham model parametr:

$$C_0 : 0.002 \frac{Ns}{m}$$

$$f_c : 0.1 N, 0.2 N$$

$$f_0 : 1$$

Figure 5.3.5 Simulation results of Bingham

To identify the Bingham parameters, it has been used the torque equation of the Magneto-rheological (MR) brake.

Torque-Angle hysteresis loop describes the displacement of the body angle between the (-3.5 , 3.5)deg.

Torque-Angular velocity hysteresis loop describes the rotational speed of the body angular velocity in deg/sec.

6 Electronic setup

The components/equipments of the electronic setup for the semi active suspension system used in this project is consist into several categories:

1. Mechanical unit: DC high torque motor with gear, eccentric wheel, car wheel, magneto rheological damper and spring.
2. Sensors: three incremental encoders.
3. Interface and power supply unit.
4. Computers system.
5. RT – DAC I/O. PWM (Pulse width modulation and encoders)

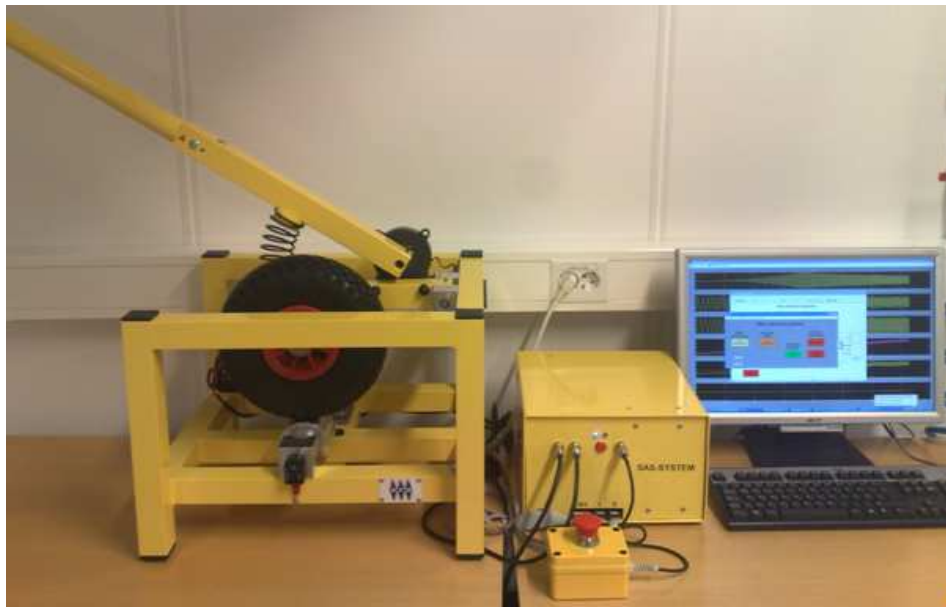


Figure 6. 1 Electronic setup of semi active suspension

6.1 Signals in/out

The input signals into magneto-rheological brake is a current by maximum 1.5Amper input .

It is the cam of the system make the equation of motion when it is in rotating, in another case it is a cam makes the system, a function of sine wave. To control current as a input signals in the SAS, it is possible to get the high or low out put torque in the MR damper. And also the system appear to the different angles (α_1 , α_2) like a out put. Here are some explain how the system works in each part.

6.1.1 Motors

The main decision in choosing motors is the maximum torque needed. The length of the arm bodies from tip to pivot is approximately one meter, so a single motor would have to generate 4 Nm that is enough the minimum requirement.

6.1.2 Cam follower system (Eccentric)

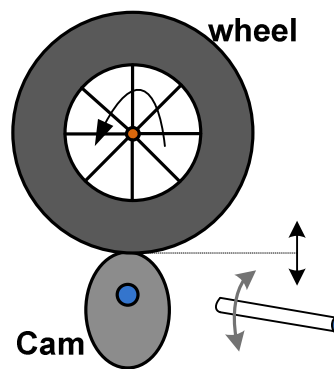


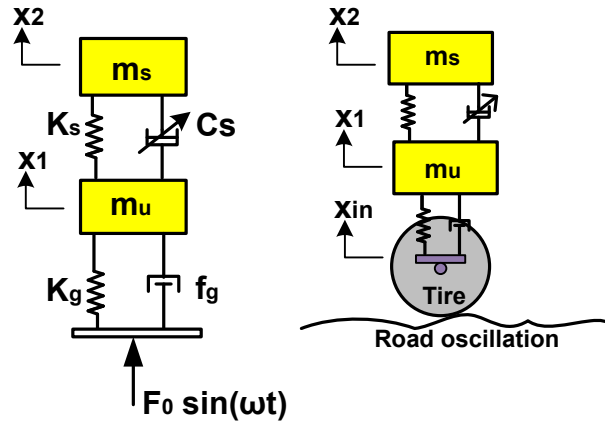
Figure 6. 2 Cam Design

All cam follower system have sufficient elasticity in their components to present the possibility of residual vibrations in operation. There are oscillations relatively from the nature, such as road oscillations, like a car body vibrations when the car hits a bump or hole during driving, or earthquake vibrations, then the semi active suspension has the ability to store energy to spring and to dissipate it through the damper.

Well in this case there is an eccentric in the quarter of car, which is connected to a motor by the shaft, and the follower of this eccentric is the tyre, which is the tyre is connected to the unsprung mass. The movement of the follower is then transmitted to another mechanism or another part of the mechanism system.

Then there is connection between the unsprung mass to the MR brake by the spring between the mass and unsprung mass. Therefore in generally, the torque of the mechanical system have a distance measurements from the body/sprung mass and unsprung mass.

The equations can be developed by means of Newton's or Lagrange's equations however, the details of the formulation have been left out and simply the respective equation of motion (EOM) has been presented.



Figur 6. 3 Quarter of car design

The model used in figure 6. 3 including sprung (m_s) and unsprung mass (m_u), linear spring stiffness (k_s), rotational damper (c) and tire stiffness (k_g). Using Newton's equations, the EOMs for the two-mass suspension model were derived in mechanical vibrations and are shown here.

$F_0 \sin(\omega t)$ is the external force, which is the function of road oscillation. The general equation of motion of the eccentricity is described of the model in figure above like a quarter a car.

$$\text{Equation of motion: } M[\ddot{X}] + C[\dot{X}] + K[X] = \{F(t)\}$$

Where the M is the mass matrix, the C is the damping matrix, and the K is the stiffness matrix for the system.

Based on equation of motion, the system is describe in below:

$$m_u \ddot{x}_1 + f_g \dot{x}_1 + k_g x_1 + c_s (\dot{x}_2 - \dot{x}_1) + k_s (x_2 - x_1) = F_0 \sin(\omega t) \quad (6.1)$$

$$m_s \ddot{x}_2 + c_s (\dot{x}_2 - \dot{x}_1) + k_s (x_2 - x_1) = 0 \quad (6.2)$$

From the equation (6.1) and (6.2) in matrix form there is:

$$\begin{bmatrix} m_u & 0 \\ 0 & m_s \end{bmatrix} \begin{bmatrix} \ddot{x}_1 \\ \ddot{x}_2 \end{bmatrix} + \begin{bmatrix} f_g + c_s & -c_s \\ -c_s & c_s \end{bmatrix} \begin{bmatrix} \dot{x}_1 \\ \dot{x}_2 \end{bmatrix} + \begin{bmatrix} k_g + k_s & -k_s \\ -k_s & k_s \end{bmatrix} \begin{bmatrix} x_1 \\ x_2 \end{bmatrix} = \begin{bmatrix} F_0 \sin(\omega t) \\ 0 \end{bmatrix}$$

The excitation is now composed of real and imaginary components. The system equation explains that how the equation of motion works in the semi active suspension system as a quarter of car body. [11]

6.1.3 Wheel

The wheel is follower of the system, which has the two degree of freedom in the system.

The rotation speed of the wheel is depends on the how fast cam is driven, by increase or decrease the current in motor. The angle of the lower beam measured by the encoder which is mounted at the lever, and it is given in degree. Also the rotation velocity of the wheel expressed in deg/sec.

6.1.4 Mass and unsprung mass

Both of the body and unsprung mass has one degree of freedom (1DF.), and it is also depends on rotation speed of wheel. If current in the motor increases, then those two bodies jumping more than they do, then angles between them is chnging.

The bodies angle of the upper beam measured by the encoder, which is mounted at the lever, given in degree. Also the bodies velocity of the upper beam expressed in deg/sec.

6.1.5 Brake

The restoring force in a Magnetorehelogical (MR) damper depends on the rotary damper velocity and the magnetic field strength. The higher the angular DC motor velocity the higher frequency of car wheel vertical oscillations. Friction damping is controlled by the increase in yield strength of the MR fluid in response to the magnetic field strength. As a magnetic field is applied to the Magnetorehelogical fluid in the MR brake, the characteristics of the fluid change to provide by increasing torque output.



Figure 6. 4 Picture of MR brake

This brake (model RD-2087-01) has 96.6 mm diameter, 43.7 mm width and can provide 4 Nm torque with (1.5 A) current input.

6.2 Connection diagram

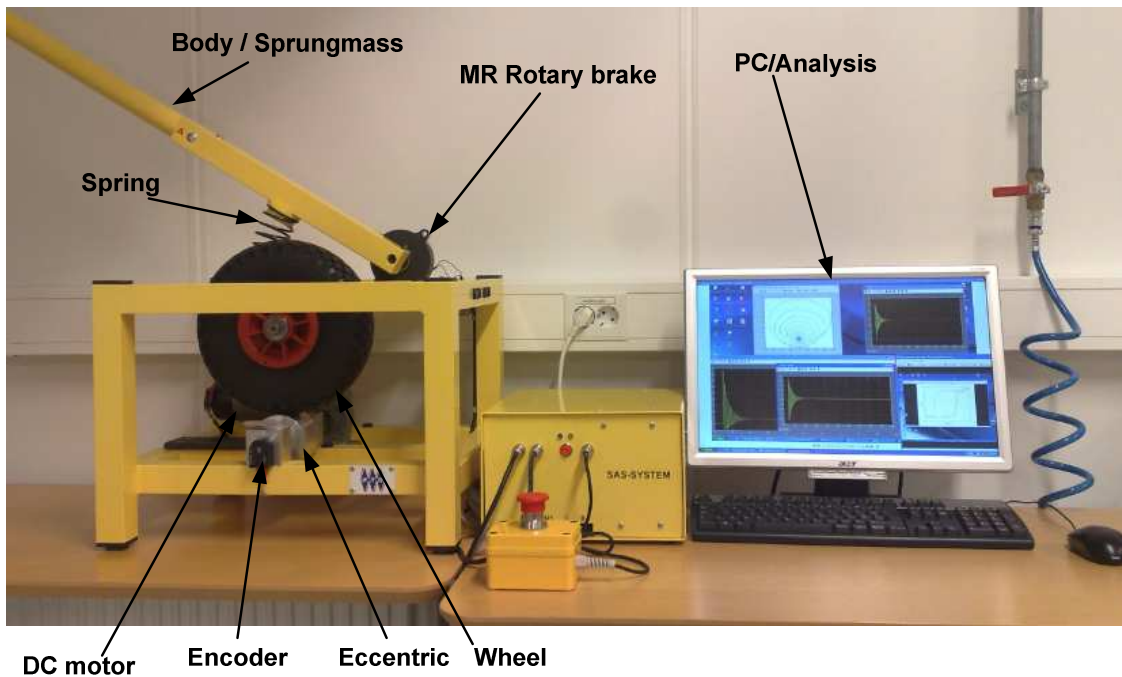
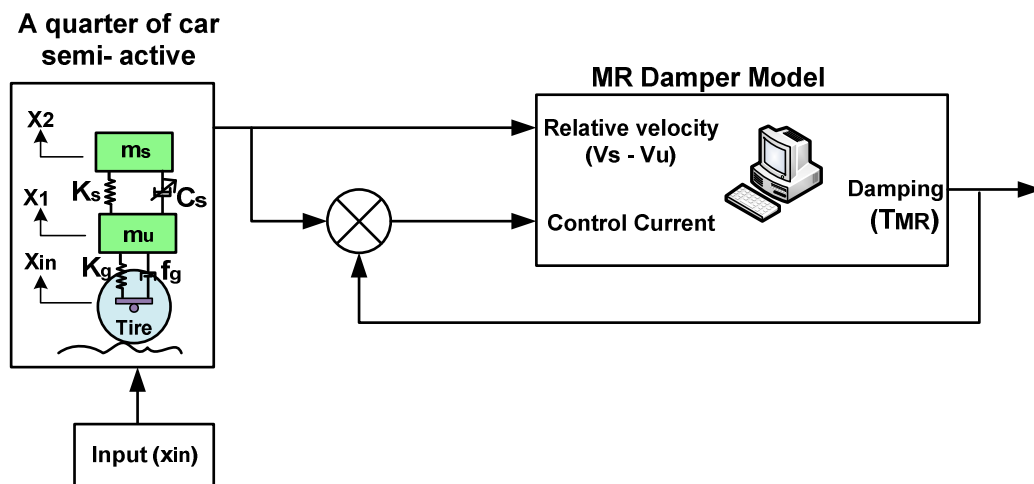


Figure 6.2.1 Prototype of the semi-active friction device

The input velocities to the MR subsystem are taken from the vehicle model and the damping T_{MR} is a feedback to the vehicle model as a torque actuator. By control the current from 0 to 1 A, it is possible to have the system in passive and semi-active system.



Figur 6.2. 2 MR Damper Feedback Control

Generally, semi active controller models have been developed base on quarter vehicle model, which requires the absolute velocites of the sprung mass and unsprung mass.

7 Software setup

7.1 Design of semi active controller

MR rotary brakes are nonlinear devices that generate hysteresis force-velocity and force-displacement response.

This nonlinear dynamics makes the application of nonlinear control techniques for reliable performance.

In this section, Back-stepping technique is used to account the nonlinearities and uncertainties of the system. The objective is to design an adaptive back-stepping controller for regulating the suspension deflection of the vehicle with the aid of an MR rotary brake. In order to formulate the control system, the dynamic motion of equations of the quarter car model. [4][8]

Consider the system: $\dot{y}_2 = f + g (T_{MR})$

$$y_1 = \alpha_2$$

$$\dot{y}_1 = y_2$$

$$y_2 = \dot{\alpha}_2$$

$$\dot{y}_2 = \frac{1}{J_2} \left(k_2 y_2 - M_2 \cos(y_1) + r_2 k_s \left(l_{0s} - \sqrt{(r_2 \cos \alpha_2 - r_1 \cos \alpha_1)^2 + (r_2 \sin \alpha_2 - r_1 \sin \alpha_1)^2} \right) \right) + \frac{1}{J_2} T_{MR}$$

$$f = \frac{1}{J_2} \left(k_2 y_2 - M_2 \cos(y_1) + r_2 k_s \left(l_{0s} - \sqrt{(r_2 \cos \alpha_2 - r_1 \cos \alpha_1)^2 + (r_2 \sin \alpha_2 - r_1 \sin \alpha_1)^2} \right) \right)$$

$$g = \frac{1}{J_2} (T_{MR})$$

Where :

$$T_{MR} = (C_0 + C_1(i)) \dot{\theta} + (\alpha_0 + \alpha_1(i)) z$$

Consider the function of the current:

$$i = - \left[\frac{(\alpha_2 - \alpha_{2eq}) + (1 + h_1 h_2) + (h_1 + h_2) \omega_2 + f - g (c_0 (\dot{\theta}) + \alpha_0 z)}{(c_1 (\dot{\theta}) + \alpha_1 z) g} \right]$$

Where:

$$\alpha_{2eq} = (-k_2 \omega_2) + (-m_u g \cos(\alpha_2))$$

h_1, h_2 : Constant value

7.2 RT (SAS)

Real time experiments

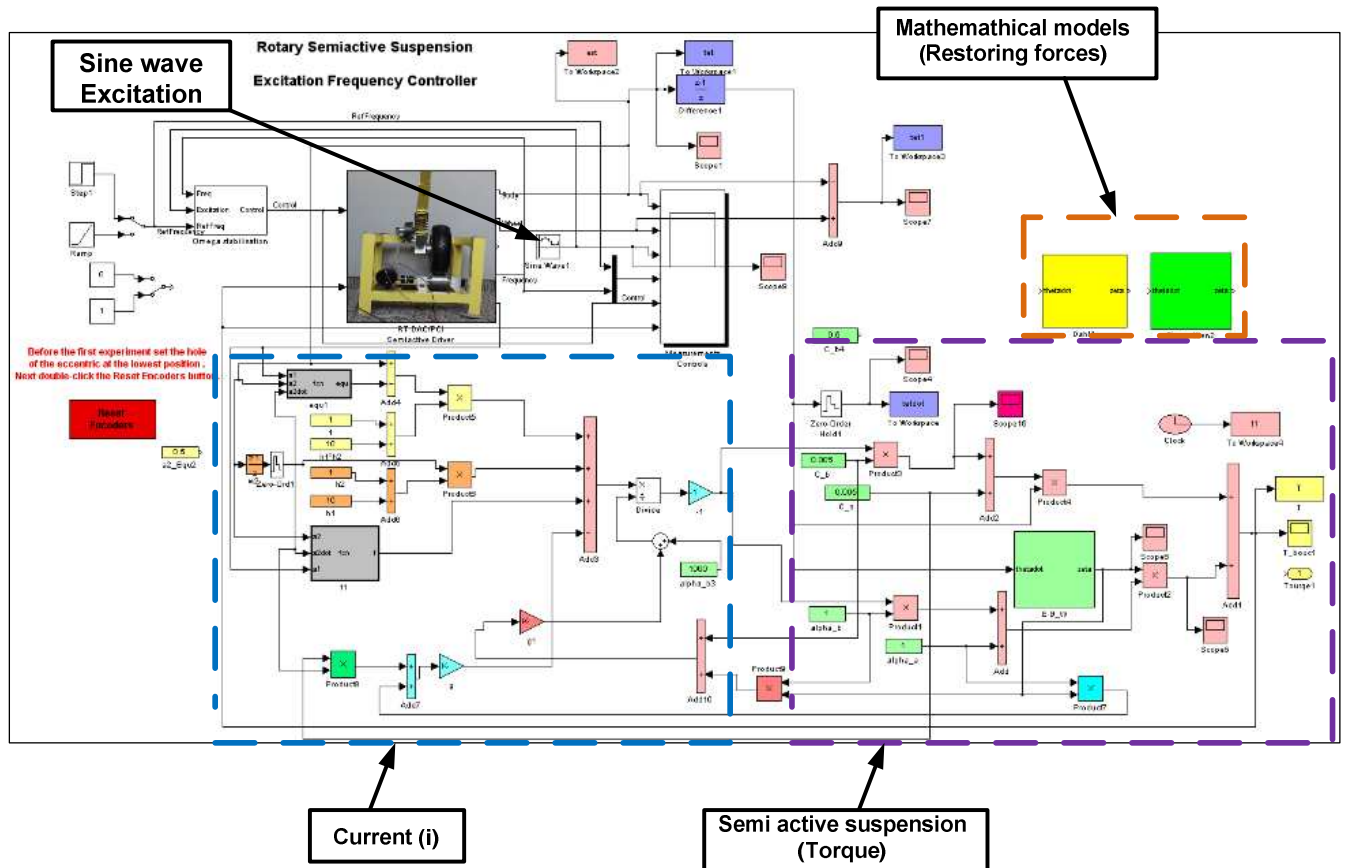


Figure 7.2.1 Real time of SAS

In the diagram presented above, apart from the SAS system control, there are included two important parts: current control and semi-active suspension. By adjusting values of the current it is possible to change the value of torque generated in the MR brake, i.e. the damping friction in the magnetorheological fluid. That torque is subsequently sent back to the SAS physical system, as its input (together with the excitation).

Sine wave is an input disturbance to the vehicle as a road oscillations, and the output is the angle of rotation of the sprung mass (car body). This angle is measured by the encoder, that is mounted to the MR rotary brake.

$$\theta = \alpha_1 - \alpha_2$$

7.3 Modules

Over view of the Semi Active Suspension system (SAS) control window

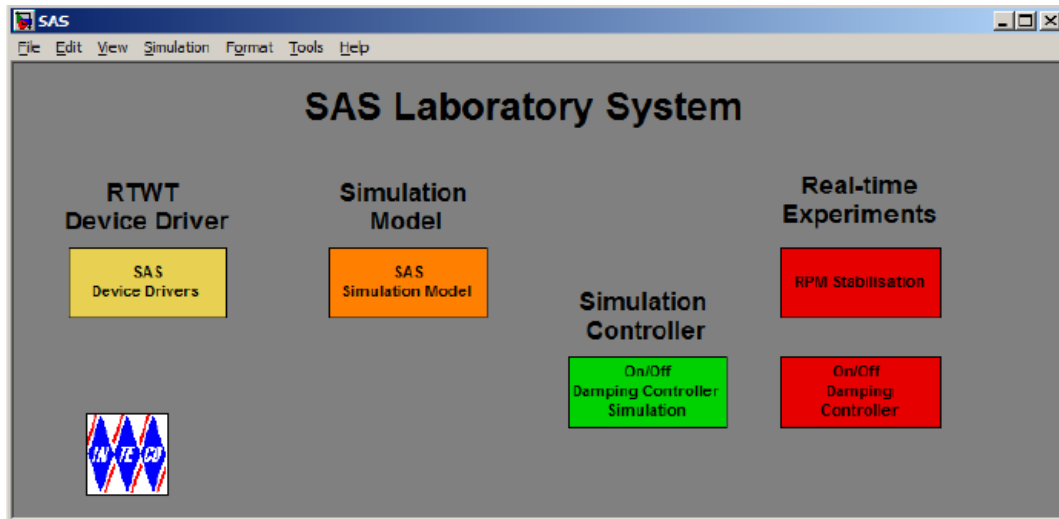


Figure 7.3.1 Control window of SAS

The SAS control windows consists in four categories:

1. RTWT device driver
2. Simulation model
3. Simulation driver
4. Real Time controllers

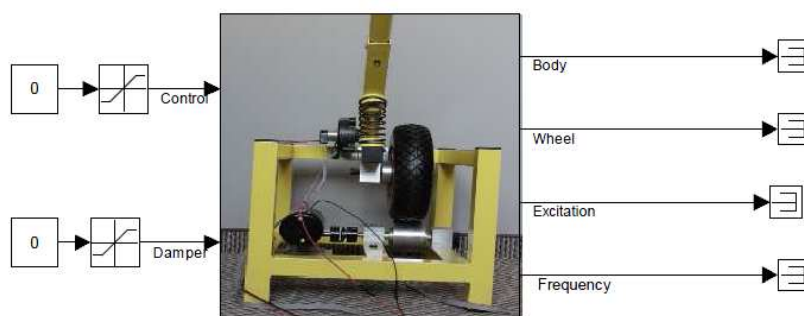


Figure 7.3. 2 Real-time Device Driver

The DC motor control and Damper are two main inputs of the device driver. Also the car body (position), wheel positin, excitation of the eccentric and frequency are four outputs of this device driver. With the fact that the excitation of the system is sine wave.

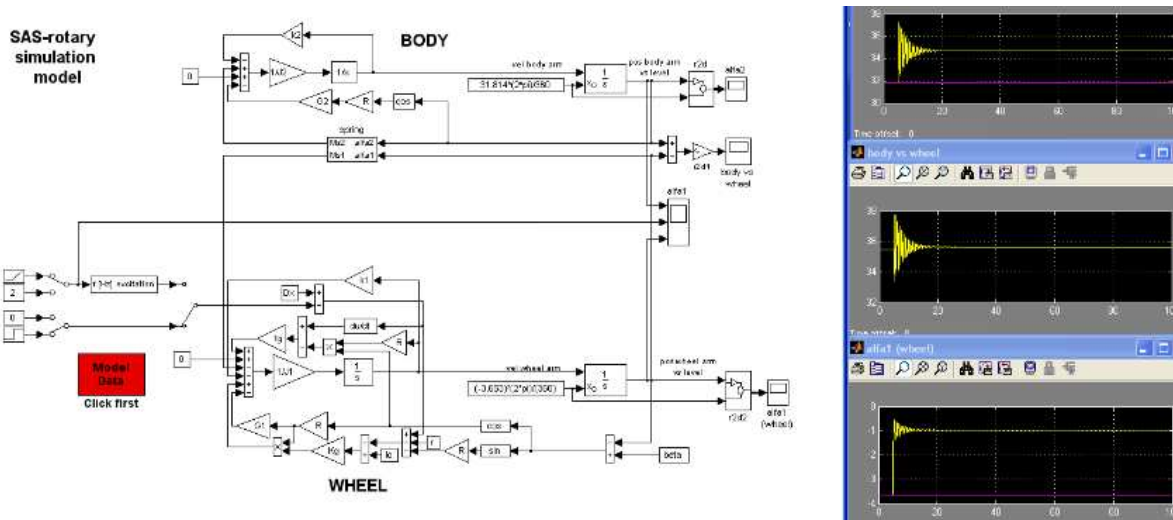


Figure 7.3. 4 Simulation model of the SAS

The simulink block diagram of the dynamic equation, which is explained in the chapter 4.3 for the mechanical system (quarter of car) was made in such a way that the angle of rotation of the body (sprung mass) and unsprung mass are outputs of the system. By this method it is possible to see the angular position of the body and unsprung mass. This is different approach than the one shown in Fig. 7.2.1, in which the output of the model is the function of MR Damper or function of restoring force.

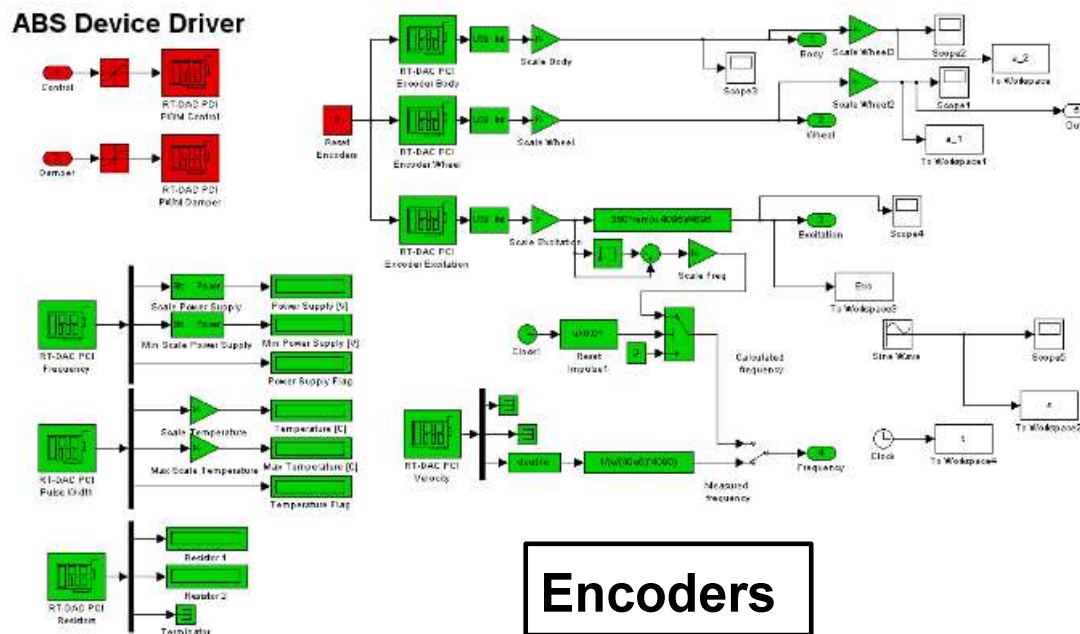


Figure 7.3. 5 ABS device Driver

ABS Device Driver is a model which is measure the angle of the body(sprung mass) and unsprung mass for the system due to the bodies vibrations.

8. Project conclusion

During this project it has been studied the vibration suppression systems, such as passive, active and semi active.

The application of the physical device for the vibration control is studied. The dynamic equation of the mechanical SAS system is derived together with the geometrical and graphical description of the system. Equations of motion are established by using Newton's 2nd law. Some interesting observations are obtained and their physical insights are explained.

The flexibility of shaping the closed-loop road excitation frequency responses of a quarter-car model by feedback control was investigated.

Physical torque equation due to the MR brake has been investigated, and then parameters of the different mathematical models have been estimated. Also, the parameters identification has been done for the real experimental data. The estimated hysteresis loops were compared in passive and semi active suspension with the real experimental results. Furthermore, it was found that the disadvantage of the passive damping strategy is that there is no control in this system, while the advantage for the semi active damping control is the fact that the value of braking torque can be changed by increasing or decreasing current.

8.1 Future work

It is recommended to further study the real experimental data of the SAS system and try to identify the parameters and optimize the hysteresis loop by using back-stepping technique. It is also advisable to evaluate the results obtained from this approach by testing those estimated parameters for different MR damper models.

Reference list

- [1] A New Structure of MR Brake with the Waveform Boundary of Rotary Disk
School of Mechanical and Automotive Engineering , University of Ulsan, Ulsan, Korea.
- [2] Modeling of a Magneto-rheological Actuator Including Magnetic Hysteresis
Department of Mechanical Engineering, Korea Advanced Institute of Science and Technology.
- [3] Magneto-Rheological Dampers for Super-sport Motorcycle Applications
Thesis submitted to the Faculty of the Virginia Polytechnic Institute and State University
In partial fulfillment of the requirements for the degree of freedom
- [4] SEMIACTIVE VIBRATION ABSORPTION IN AIRCRAFT LANDING GEARS USING
MAGNETORHEOLOGICAL DAMPERS. Program “Informàtica Industrial i Automàtica”
Girona, Spain JULY, 2009
- [5] PASSIVE AND SEMI-ACTIVE TUNED MASS DAMPER BUILDING SYSTEMS
University of Canterbury, Christchurch, New Zealand2007
- [6] VIBRATION CONTROL OF CIVIL ENGINEERING STRUCTURES
Ningsu Luo University of Girona, Spain
- [7] Simulation of Magnetic Fields in a Generator for an MR Rotary Damper Using COMSOL
Multiphysics
- [8] Vibration Absorption in Automotive and Aeronautic Systems by Using Semiactive
Suspension with Magnetorheological Dampers. Ningsu Luo, Mauricio Zapateiro, Irene
RomeroInstitute of Informatics and ApplicationsUniversity of Girona, Campus Montilivi,
P417003 Girona, Spain.
- [9] IDENTIFICATION OF NON-LINEAR HYSTERETIC ISOLATORS FROM PERIODIC
VIBRATION TESTS. *Department of Civil and Structural Engineering\ The Hong Kong
Polytechnic University\ Kowloon\ Hong Kong*
- [10] A haptic interface for a virtual drum-kit
Peter BennettMEng Cybernetics, University of Reading
- [11] IMPROVING THE PERFORMANCE OF THE SEMI-ACTIVE TUNED MASS DAMPER
Academic dissertation to be presented with the assent of the Faculty of Technology of the
University of Oulu for public defence in Raahensali (Auditorium L10), Linnanmaa, on 29
May 2009